Table 2 Distribution of the c.14576G>A variant among patients with MMD, parents of the patients, and normal control Japanese individuals[a]

		c.14576G>A genotype			
	Total	Wild-type: G/G (%)	Heterozygous: G/A (%)	Homozygous: A/A (%)	GA + A/A (%)
Patients with MMD	204	36 (17.6)	153 (75.0)	15 (7.4)	168 (82.4)
Sporadic	163	34 (20.8)	117 (71.8)	12 (7.4)	129 (79.2)
With no other variant	137	20 (14.6)	105 (76.6)	12 (8.8)	117 (85.4)
With one other variant	25	13 (52)	12 (48)	0	12 (48)
With one other homozygous variants	1	1 (100)	0	0	0
Familial	41	2 (4.9)	36 (87.8)	3 (7.3)	39 (95.1)
With no other variant	36	0	33 (91.7)	3 (8.3)	36 (100)
With one other variant	3	0	3 (100)	0	3 (100)
With 2 other compound heterozygous variants	2	2 (100)	0	0	0
Parents of patients with MMD	141	77 (54.6)	63 (44.7)	1 (0.7)	64 (45.4)
Affected	9	0	8 (88.9)	1 (11.1)	9 (100)
Unaffected	132	77 (58.3)	55 (41.7)	0	55 (41.7)
Normal controls	283	278 (98.2)	5 (1.8)	0	5 (1.8)
OR (patients with MMD vs normal control)			236	ND	259
95% CI			91-615		100-674
p (Fisher exact test)			<0.001	<0.001	<0.001

Abbreviations: CI = confidence interval; MMD = moyamoya disease; ND = not determined; OR = odds ratio.
[a] Numbers of patients in each category (%) are shown.

283 normal control Japanese individuals (1.8%) (table 2 and table e-1). Sixty-two pairs of parents were also tested for the c.14576G>A genotype, with the conclusion that the c.14576G>A variant allele was inherited from either or both parents in all patients tested. Among 168 patients with the c.14576G>A variant, 15 had a homozygous change, whereas none of the controls and unaffected parents did. We conclude that the heterozygous c.14576G>A variant increases the risk for MMD with an odds ratio (OR) of 236 (95% CI 91–615, $p < 0.001$). Because no homozygous mutation was detected in the control samples or unaffected family members, the OR for the homozygote could not be calculated (∞), suggesting its strong effect. The incidence rate of MMD was calculated to be extremely high with a 95% CI of 0.78–1.00 with the homozygous mutation. Eighteen other genetic variants beside c.14576G>A were also identified in *RNF213* (figure 1, table e-1). Sixteen of them were novel, which had not been reported in the previous studies.[14,15] Two of the variants were also found in the previous study[14]; however, they were thought to be common single nucleotide polymorphisms because they were also found in the normal controls without the significant difference of frequency. Other genetic variants showed a relatively small OR without any significance (table e-1). Thirty-one patients had these individual variants (table 2). Fifteen of them also had the heterozygous c.14576G>A, and 4 of 5 patients whose parents' samples were available had these 2 variants existing as compound heterozygotes (for example, one variant from the father and the other from the mother). In the other 16 patients having no c.14576G>A, 1 had a homozygous c.13342G>A variant, and 2 had 2 variants: c.13342G>A and c.14053G>A as a compound heterozygote. Of the novel 16 variants, 11 of them were not found in 188 normal control Japanese individuals and were all private mutations (only once in one family).

Correlation between the c.14576G>A genotype and clinical phenotype. We compared the clinical features of patients with MMD according to the c.14576G>A genotype, the wild type (genotype GG, as group GG), the heterozygote (genotype GA, as group GA), or the mutant homozygote (genotype AA, as group AA). Age at onset was lower in AA than in GA or GG ($p = 0.002$ or $p = 0.007$) (figure 2A and table e-2). Median age at onset was 3 years in AA, 7 years in GA, and 8 years in GG. Among those with childhood onset (age at onset <15 years), in whom the effect of secondary vascular changes in later life could be ignored and therefore a pure genetic effect could be expected, the association between earlier onset age and the homozygous c.14576G>A genotype was clearly replicated (table e-2). Although the clinical manifestation is different

Figure 1 Schematic diagram of the RNF213 protein and genomic structure of *RNF213*

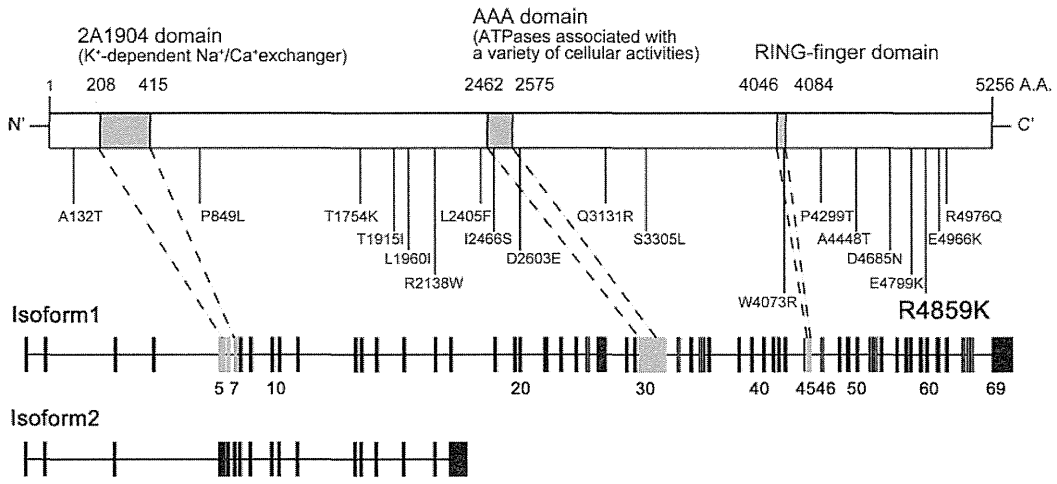

A schematic presentation of the RNF213 protein with 3 conserved domains, the genetic variants we have identified, and the genomic structures of 2 *RNF213* isoforms (shown from top to bottom). All missense changes, including R4859K (c.14576G>A as larger characters) are indicated. A.A. = amino acids; AAA = ATPases associated with a variety of cellular activities; RING = really interesting new gene. (Based on National Center for Biotechnology Information Reference sequence, NP_065965.4.)

between the childhood-onset group and the adult-onset group, the rates of the patients with this variant, 83.2% (119 of 143 patients) and 79.6% (43 of 54 patients), respectively, were not significantly different. Among adult patients, there was no significant difference in the rate of having this variant between those with familial history (84.6%, 11 of 13 patients) and those without (78.0%, 32 of 41 patients). The univariate Cox regression analysis showed that only the c.14576G>A genotype was the significant predictive variable for age at onset (table e-4). The cumulative incidence of MMD was higher in AA than GA or GG at almost all age distributions (figure 2B), but this tendency was more apparent in the childhood-onset group. Further investigation with more AA and GG patients is necessary for better statistical accuracy. More AA patients were affected before age 4, compared with GA and GG patients ($p < 0.001$) (figure 3A). All AA patients had infarctions at initial presentation.

Figure 2 Correlation between the c.14576G>A variant and age at onset

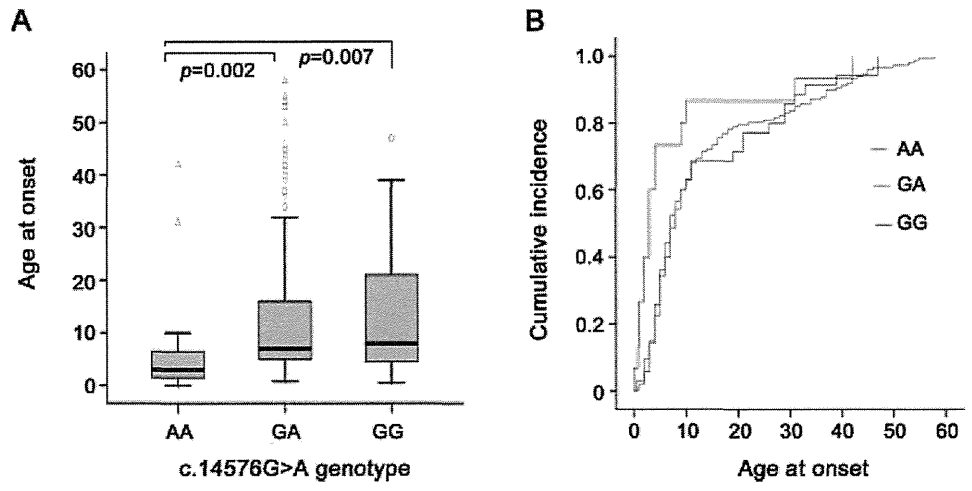

(A) A box plot of age at onset between 3 groups of patients with either the mutant homozygote (AA), heterozygote (GA), or wild type (GG) of the c.14576G>A variant. ○ indicates mild outliers; △ indicates extreme outliners. (B) Cumulative incidence curve of the 3 groups of patients with either the mutant homozygote (AA), heterozygote (GA), or wild type (GG) of the c.14576G>A variant.

Figure 3 Correlation between c.14576G>A variant and clinical features

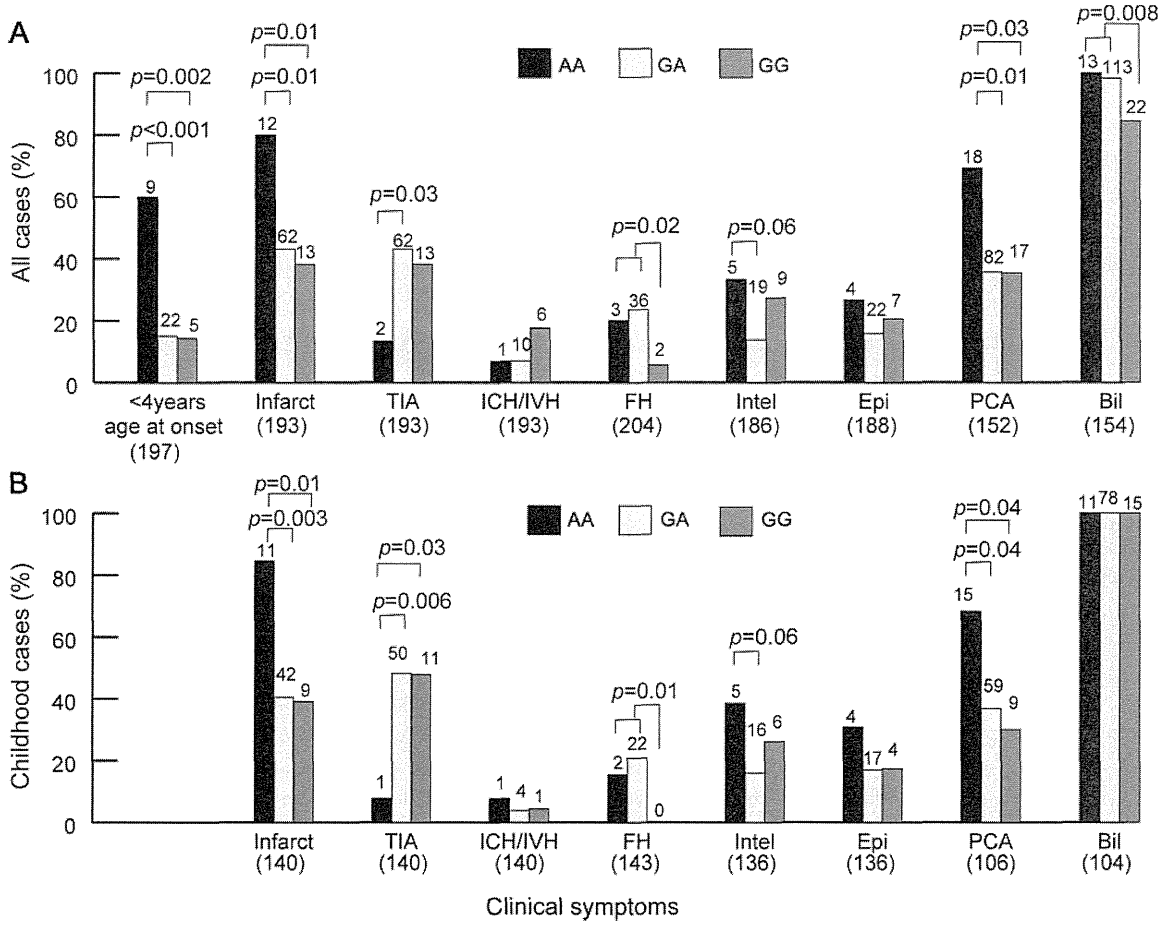

(A) The clinical characteristics of MMD for the 3 groups of patients with either the mutant homozygote (AA), heterozygote (GA), or wild type (GG) of the c.14576G>A variant (204 patients). The numbers of total patients with clinical records regarding either the presence or absence of each characteristic are indicated below the bars, and the numbers of patients in each group are indicated above the respective bars. (B) Clinical characteristics of MMD for the 3 groups of patients with either the mutant homozygote (AA), heterozygote (GA), or wild type (GG) of the c.14576G>A variant among those with age at onset younger than 15 years. The numbers of total patients with clinical records regarding either the presence or absence of each characteristic are indicated below the bars, and the numbers of patients in each group are indicated above the respective bars. Bil = bilateral vasculopathy; Epi = epilepsy; FH = with family history; ICH/IVH = intracranial hemorrhage/intraventricular hemorrhage, Infarct = infarction; Intel = intellectual impairment; PCA = posterior cerebral artery involvement.

The frequencies of other clinical features of MMD in AA, GA, and GG were also compared (figure 3A and table e-2). As the clinical manifestation at diagnosis, infarction was more common in AA than in GA or GG ($p = 0.01$, OR 5.3, 95% CI 1.43–19.56 or $p = 0.01$, OR 6.5, 95%CI 1.53–27.32); TIA was less common in AA than in GA ($p = 0.03$; OR 0.20; 95% CI 0.04–0.94). Bilateral MMD and family history of the disease were more frequent in AA and GA than in GG ($p = 0.008$, OR 11, 95% CI 1.98–66.36 and $p = 0.02$, OR 5.1, 95% CI 1.18–22.36). The number of steno-occlusive PCAs was larger in AA than in GA ($p = 0.01$) (counted as 2 arteries per person). Seventy-four of the 152 patients (48.6%) had PCA lesions, and infarctions and intellectual impairment were more frequent in those with PCA involvement than those without (infarctions 68.9% vs 30.8%, $p < 0.001$; intellectual impairment 26.8% vs 5.3%, $p < 0.001$). Intellectual impairment and epilepsy tended to be a more common complication in AA than in GA, with and without marginal significance. We also compared these clinical features in AA, GA, and GG, excluding 6 patients with unilateral MMD, but the results were not changed (data not shown). Among childhood-onset cases (age at onset <15 years), the associations between the c.14576G>A genotype and these clinical features were generally similar, except for bilateral vasculopathy (all genotypes in childhood-onset cases showed bilateral involvement) (figure 3B).

Correlation between variants other than c.14576G>A and clinical phenotype. We also compared the clinical features of patients with MMD with the other variants, except the c.14576G>A variant, with those without (table e-3). Interestingly, none of the c.14576G>A homozygotes had any other variants. The other patients were categorized into 4 groups, who showed at least one of any individual variants without c.14576G>A (as group GG1), no other variant without c.14576G>A (as group GG0), at least one of any other variants with heterozygous c.14576G>A (as group GA1), and no other variant with heterozygous c.14576G>A (as group GA0). Although there were no differences in age at onset between GG1 and GG0 patients, it was lower in GA0 patients than GA1 patients ($p = 0.03$). Median age at onset was 7 years for GA0 and 12 years for GA1. The frequency of infarctions was lower and that of intracerebral hemorrhage was higher in GA1 than in GA0 ($p = 0.02$, OR 0.19, 95% CI 0.04–0.90 and $p = 0.009$, OR 8.3, 95% CI 2.00–34.19). However, when patients with MMD with another variant, which was predicted to be pathogenic by PolyPhen-2[18] or SIFT[19] algorithms, were compared with those without, consistently no differences in any of these clinical features were observed (data not shown). Further analyses with larger numbers of patients are needed to validate this effect.

Anticipation of MMD. In addition, statistical comparisons of clinical features between 5 parent-offspring pairs having the same *RNF213* genotype (heterozygous c.14576G>A) were performed (table e-5). Age at onset was lower in the second generation than in the first generation ($p = 0.04$). Median age at onset was 5 and 37 years, respectively. This result may support the anticipation of MMD as reported previously.[13] Conversely, age at onset was not different between 6 sibling pairs having the same *RNF213* genotype ($p = 0.67$). Median age at onset was 8 years for the older siblings and 12.5 years for the younger ones. There were no differences in other clinical symptoms among patients from the same pedigree.

DISCUSSION We confirmed a strong association between c.14576G>A in *RNF213* and MMD with the larger number of Japanese patients different from those of the previous studies.[14,15] More importantly, this is the first report showing the significant phenotype-genotype correlation. The OR for the heterozygous c.14576G>A was 236 ($p < 0.001$) and could not be exactly calculated for the homozygote (∞). With the assumption that the effects of both heterozygous and homozygous changes on MMD onset were similar, the homozygous c.14576G>A variant would increase the risk with an OR of 259 (95% CI 100–674, $p < 0.001$). However, the effect of the homozygous variant on MMD onset was expected to be much larger than that of the heterozygote because no homozygote was found in a total of 283 normal controls and 132 unaffected family members in this study and 429 normal controls and 28 unaffected family members in the previous study.[14] We also showed that the risk of being diagnosed with MMD with the homozygous variant was more than 78%. Although this variant does not exactly fit the pure Mendelian inheritance pattern because it is observed to some extent in the normal population, this variant might have a much larger effect on the pathogenesis of MMD than the common variants of complex diseases, considering its extremely high OR. This rare variant could be an example of missing heritability, that is, the majority of heritability of complex traits that are unexplained by common variants with a small effect size.[20,21] Thus, this variant should not be considered as one of common variants contributing to common diseases.

The c.14576G>A variant has not been found among the total number of 55 Caucasian patients in the previous studies on *RNF213*.[14,15] However, 4 other rare variants were identified in 4 of 50 Caucasian patients.[15] The overall variant detection rate for *RNF213* was as high as 90.2% for our Japanese patients, in contrast to 8% for the Caucasian patients in the previous study.[15] Importantly, 82.4% of our patients were accounted for by the c.14576G>A variant. It was reported that c.14576G>A variant was identified in 90% of Japanese patients, 79% of Korean patients, and 23% of Chinese patients.[15] The founder effect widely distributed in some areas of east Asia was likely to be expected, and this variant could explain the difference of prevalence of MMD between Asian and non-Asian populations.

RNF213 is a RING (really interesting new gene) finger protein containing an AAA (ATPases associated with variety of a cellular activities) domain, indicating that it has E3 ubiquitin ligase activity and energy-dependent unfoldase activity.[14,22] Knockdown of *RNF213* in zebrafish leads to the abnormal sprouting and irregular diameter of intracranial vessels, suggesting its possible contribution to vascular formation.[15] More research on its contribution to MMD pathogenesis will be necessary.

Although the number of adult-onset cases was relatively small, the similar rates of the cases with this variant between childhood-onset patients and sporadic adult-onset patients might suggest that the variant apparently contributes to both groups. Either a heterozygous or homozygous c.14576G>A variant increased the risk for adult-onset MMD (OR 217,

95% CI 72–656, $p < 0.001$) compared with that in adult normal controls.

Whether bilateral and unilateral MMD belong to a single entity is a very important question. Of the 6 patients with unilateral MMD, 2 were heterozygotes and the others were wild types, which indicated a lower frequency of heterozygotes than that in the previous study.[14] Because we showed a significant difference in the frequency of bilateral vasculopathy between GG and other genotypes, we speculate that to some extent patients with unilateral MMD share a genetic background, but there could be different genetic backgrounds in these groups. Further investigation is needed to confirm these findings with larger numbers of patients with unilateral MMD.

The recent spread of brain check-up has increased the opportunity to encounter patients with asymptomatic MMD.[23] Whereas our patients in this study all had symptomatic MMD, it is necessary to further examine the *RNF213* variant in the asymptomatic group.

The homozygous c.14576G>A variant carriers showed significantly earlier age at onset, more frequent occurrence of infarctions at initial presentation, and PCA involvement. The association of PCA involvement and infarction or intellectual impairment in our data were compatible with the previous report.[11] These features indicate that c.14576G>A homozygotes have more severe and wider vasculopathy in the brain. The other poor prognostic factors, such as intellectual impairment and epilepsy,[8] were probably more frequent in homozygotes but did not reach statistical significance. We speculated that these conditions might be modified or prevented by early diagnosis and by surgical and medical interventions.

Early surgery for young patients with MMD (<3–4 years of age) has been recommended previously,[24] because they often demonstrate a more severe clinical course.[9,10,24] Approximately 80% of these patients had infarction at initial presentation and had subsequent preoperative infarctions more frequently than patients with older age at onset.[24,25] In our study, 77.1% of the patients diagnosed before age 4 had infarctions at diagnosis, whereas 38% of those diagnosed after age 4 had infarctions ($p < 0.001$), results similar to the previous data.

Conversely, it was demonstrated that young age at onset of symptoms did not always herald a poor later outcome. Instead, neurologic deficits due to infarctions at the time of surgery held the most prognostic value.[7,26] It was recently reported that an irreversible infarction was the greatest risk for an unfavorable outcome by multivariate logistic regression analysis.[8] Specific biomarkers, which might be strongly associated with infarction, would be of invaluable clinical importance to provide the appropriate timing for an operation. In our study, 60% of homozygous c.14576G>A individuals were diagnosed with MMD before age 4, and all of them had infarctions at initial presentation. Thus, the homozygous c.14576G>A variant may be a more specific predictor, which would discriminate those with poor prognosis from those with relatively favorable prognosis among patients with young-onset MMD.

We therefore propose that the homozygous c.14576G>A genotype could be an efficient DNA marker predicting the severe type of MMD with a poor prognosis and a strong biomarker for patients requiring early operation. c.14576G>A genotyping could also be useful to predict the actual risk of severe initial infarctions. Careful follow-up of these high-risk homozygotes could make it possible to undertake intervention before the first infarctions and prevent the irreversible neurologic deficits that can occur in these patients. Thus, the homozygous c.14576G>A variants may provide a better monitoring and prevention strategy. Furthermore, this variant could be very useful in genetic counseling.

AUTHOR CONTRIBUTIONS

Dr. Miyatake: study concept and design, analysis of the genetic data, data integrity, interpretation of the data, statistical analysis, and drafting/revising the manuscript. Dr. Miyake: data integrity, interpretation of the data, and drafting/revising the manuscript. Dr. Touho: analysis of the clinical data and sample collection. Dr. Nishimura-Tadaki: analysis of the genetic data. Dr. Kondo: analysis of the genetic data. Dr. Okada: analysis of the genetic data. Dr. Tsurusaki: analysis of the genetic data. Dr. Doi: analysis of the genetic data. Dr. Sakai: analysis of the genetic data. Dr. Saitsu: data integrity, interpretation of the data, and drafting/revising the manuscript. Dr. Shimojima: analysis of the clinical data and sample collection. Dr. Yamamoto: analysis of the clinical data and sample collection. Dr. Higurashi: analysis of the clinical data and sample collection. Dr. Kawahara: analysis of the clinical data, sample collection, and drafting/revising the manuscript. Dr. Kawauchi: analysis of the clinical data and sample collection. Dr. Nagasaka: analysis of the clinical data and sample collection. Dr. Okamoto: analysis of the clinical data and sample collection. Dr. Mori: analysis of the clinical data and sample collection. Dr. Koyano: analysis of the clinical data and sample collection. Dr. Kuroiwa: analysis of the clinical data and sample collection. Dr. Taguri: statistical analysis and drafting/revising the manuscript. Dr. Morita: statistical analysis and drafting/revising the manuscript. Dr. Matsubara: drafting/revising the manuscript. Dr. Kure: drafting/revising the manuscript. Dr. Matsumoto: study concept and design, analysis of the genetic data, data integrity, interpretation of the data, statistical analysis, and drafting/revising the manuscript.

ACKNOWLEDGMENT

The authors thank all the participants for their cooperation in this research; Dr. M. Amamoto, MD, from the Department of Pediatrics, Kitakyushu City Yahata Hospital Critical Care Medical Center, for providing a sample and clinical information for the patient with MMD; and Y. Yamashita, Dr. K. Nishiyama, K. Takabe, T. Miyama, and E. Koike, from the Department of Human Genetics, Yokohama City University Graduate School of Medicine, for their technical assistance.

DISCLOSURE

Dr. Miyatake reports no disclosures. Dr. Miyake is funded by research grants from the Ministry of Health, Labour and Welfare, and a Grant-in-Aid for Young Scientists from the Japan Society for the Promotion of Science. Dr. Touho, Dr. Nishimura-Tadaki, Dr. Kondo, Dr. Okada, Dr. Tsurusaki, Dr. Doi, and Dr. Sakai report no disclosures. Dr. Saitsu is funded by research grants from the Ministry of Health, Labour and Welfare and a Grant-in-Aid for Young Scientists from the Japan Society for the Promotion of Science. Dr. Shimojima reports no disclosures. Dr. Yamamoto is funded by a research grant, Scientific Research (c) from the Japan Ministry of Education, Science, Sports and Culture. Dr. Higurashi, Dr. Kawahara, Dr. Kawauchi, Dr. Nagasaka, Dr. Okamoto, Dr. Mori, Dr. Koyano, Dr. Kuroiwa, Dr. Taguri, Dr. Morita, Dr. Matsubara, and Dr. Kure report no disclosures. Dr. Matsumoto serves on editorial advisory boards for *Clinical Genetics*, *Journal of Human Genetics*, and *American Journal of Medical Genetics Part A* and is funded by research grants from the Ministry of Health, Labour and Welfare, the Japan Science and Technology Agency, a Grant-in-Aid for Scientific Research on Innovative Areas-(Foundation of Synapse and Neurocircuit Pathology)-from the Ministry of Education, Culture, Sports, Science and Technology of Japan, a Grant-in-Aid for Scientific Research from the Japan Society for the Promotion of Science, and a grant from the Takeda Science Foundation.

Received August 6, 2011. Accepted in final form October 26, 2011.

REFERENCES

1. Bigi S, Fischer U, Wehrli E, et al. Acute ischemic stroke in children versus young adults. Ann Neurol 2011;70:245–254.
2. Mackay MT, Wiznitzer M, Benedict SL, Lee KJ, Deveber GA, Ganesan V. Arterial ischemic stroke risk factors: the International Pediatric Stroke Study. Ann Neurol 2011; 69:130–140.
3. Wakai K, Tamakoshi A, Ikezaki K, et al. Epidemiological features of moyamoya disease in Japan: findings from a nationwide survey. Clin Neurol Neurosurg 1997;99(suppl 2):S1–S5.
4. Kuriyama S, Kusaka Y, Fujimura M, et al. Prevalence and clinicoepidemiological features of moyamoya disease in Japan: findings from a nationwide epidemiological survey. Stroke 2008;39:42–47.
5. Yonekawa Y, Ogata N, Kaku Y, Taub E, Imhof HG. Moyamoya disease in Europe, past and present status. Clin Neurol Neurosurg 1997;99(suppl 2):S58–S60.
6. Kuroda S, Houkin K. Moyamoya disease: current concepts and future perspectives. Lancet Neurol 2008;7:1056–1066.
7. Scott RM, Smith ER. Moyamoya disease and moyamoya syndrome. N Engl J Med 2009;360:1226–1237.
8. Kim SK, Cho BK, Phi JH, et al. Pediatric moyamoya disease: an analysis of 410 consecutive cases. Ann Neurol 2010;68:92–101.
9. Karasawa J, Touho H, Ohnishi H, Miyamoto S, Kikuchi H. Long-term follow-up study after extracranial-intracranial bypass surgery for anterior circulation ischemia in childhood moyamoya disease. J Neurosurg 1992; 77:84–89.
10. Kurokawa T, Tomita S, Ueda K, et al. Prognosis of occlusive disease of the circle of Willis (moyamoya disease) in children. Pediatr Neurol 1985;1:274–277.
11. Yamada I, Himeno Y, Suzuki S, Matsushima Y. Posterior circulation in moyamoya disease: angiographic study. Radiology 1995;197:239–246.
12. Yamauchi T, Houkin K, Tada M, Abe H. Familial occurrence of moyamoya disease. Clin Neurol Neurosurg 1997; 99(suppl 2):S162–S167.
13. Nanba R, Kuroda S, Tada M, Ishikawa T, Houkin K, Iwasaki Y. Clinical features of familial moyamoya disease. Childs Nerv Syst 2006;22:258–262.
14. Kamada F, Aoki Y, Narisawa A, et al. A genome-wide association study identifies RNF213 as the first moyamoya disease gene. J Hum Genet 2011;56:34–40.
15. Liu W, Morito D, Takashima S, et al. Identification of RNF213 as a susceptibility gene for moyamoya disease and its possible role in vascular development. PLoS One 2011; 6:e22542.
16. Fukui M. Guidelines for the diagnosis and treatment of spontaneous occlusion of the circle of Willis ('moyamoya' disease): Research Committee on Spontaneous Occlusion of the Circle of Willis (Moyamoya Disease) of the Ministry of Health and Welfare. Japan Clin Neurol Neurosurg 1997;99(suppl 2):S238–S240.
17. Garritano S, Gemignani F, Voegele C, et al. Determining the effectiveness of high resolution melting analysis for SNP genotyping and mutation scanning at the TP53 locus. BMC Genet 2009;10:5.
18. Adzhubei IA, Schmidt S, Peshkin L, et al. A method and server for predicting damaging missense mutations. Nat Methods 2010;7:248–249.
19. Ng PC, Henikoff S. SIFT: predicting amino acid changes that affect protein function. Nucleic Acids Res 2003;31: 3812–3814.
20. Eichler EE, Flint J, Gibson G, et al. Missing heritability and strategies for finding the underlying causes of complex disease. Nat Rev Genet 2010;11:446–450.
21. Manolio TA, Collins FS, Cox NJ, et al. Finding the missing heritability of complex diseases. Nature 2009;461: 747–753.
22. Lupas AN, Martin J. AAA proteins. Curr Opin Struct Biol 2002;12:746–753.
23. Ikeda K, Iwasaki Y, Kashihara H, et al. Adult moyamoya disease in the asymptomatic Japanese population. J Clin Neurosci 2006;13:334–338.
24. Kim SK, Seol HJ, Cho BK, Hwang YS, Lee DS, Wang KC. Moyamoya disease among young patients: its aggressive clinical course and the role of active surgical treatment. Neurosurgery 2004;54:840–844.
25. Mugikura S, Higano S, Shirane R, Fujimura M, Shimanuki Y, Takahashi S. Posterior circulation and high prevalence of ischemic stroke among young pediatric patients with Moyamoya disease: evidence of angiography-based differences by age at diagnosis. AJNR Am J Neuroradiol 2011;32:192–198.
26. Scott RM, Smith JL, Robertson RL, Madsen JR, Soriano SG, Rockoff MA. Long-term outcome in children with moyamoya syndrome after cranial revascularization by pial synangiosis. J Neurosurg 2004;100:142–149.

OPEN ACCESS Freely available online PLoS one

Screening of *MAMLD1* Mutations in 70 Children with 46,XY DSD: Identification and Functional Analysis of Two New Mutations

Nicolas Kalfa[1,2], Maki Fukami[3], Pascal Philibert[1], Francoise Audran[1], Catherine Pienkowski[4], Jacques Weill[5], Graziella Pinto[6], Sylvie Manouvrier[7], Michel Polak[6], Totsumo Ogata[3], Charles Sultan[1,2,8]*

1 Service d'Hormonologie, Hôpital Lapeyronie, CHU de Montpellier et UM1, Montpellier, France, **2** Service de Chirurgie et Urologie Pédiatrique, Hôpital Lapeyronie, CHU de Montpellier et UM1, Montpellier, France, **3** Department of Molecular Endocrinology, National Research Institute for Child Health and Development, Tokyo, Japan, **4** Unité d'Endocrinologie Pédiatrique, Hôpital des Enfants, CHU de Toulouse, Toulouse, France, **5** Clinique de Pédiatrie, Hôpital Jeanne de Flandre, CHU de Lille, Lille, France, **6** Unité d'Endocrinologie Pédiatrique, Hôpital Necker Enfants Malades, APHP, Paris, France, **7** Service de Génétique Clinique, Hôpital Jeanne de Flandre, CHU de Lille, Lille, France, **8** Unité d'Endocrinologie et Gynécologie Pédiatriques, Service de Pédiatrie, Hôpital Arnaud de Villeneuve et UM1, CHU de Montpellier, Montpellier, France

Abstract

More than 50% of children with severe 46,XY disorders of sex development (DSD) do not have a definitive etiological diagnosis. Besides gonadal dysgenesis, defects in androgen biosynthesis, and abnormalities in androgen sensitivity, the Mastermind-like domain containing 1 (*MAMLD1*) gene, which was identified as critical for the development of male genitalia, may be implicated. The present study investigated whether *MAMLD1* is implicated in cases of severe 46,XY DSD and whether routine sequencing of *MAMLD1* should be performed in these patients. Seventy children with severe non-syndromic 46,XY DSD of unknown etiology were studied. One hundred and fifty healthy individuals were included as controls. Direct sequencing of the *MAMLD1, AR, SRD5A2* and *NR5A1* genes was performed. The transactivation function of the variant *MAMLD1* proteins was quantified by the luciferase method. Two new mutations were identified: p.S143X (c.428C>A) in a patient with scrotal hypospadias with microphallus and p.P384L (c.1151C>T) in a patient with penile hypospadias with microphallus. The *in vitro* functional study confirmed no residual transactivating function of the p.S143X mutant and a significantly reduced transactivation function of the p.P384L protein ($p = 0.0032$). The p.P359S, p.N662S and p.H347Q variants are also reported with particularly high frequency of the p.359T- p.662G haplotype in the DSD patients. Severe undervirilization in XY newborns can reveal mutations of *MAMLD1*. *MAMLD1* should be routinely sequenced in these patients with otherwise normal *AR, SRD5A2* and *NR5A1*genes.

Citation: Kalfa N, Fukami M, Philibert P, Audran F, Pienkowski C, et al. (2012) Screening of *MAMLD1* Mutations in 70 Children with 46,XY DSD: Identification and Functional Analysis of Two New Mutations. PLoS ONE 7(3): e32505. doi:10.1371/journal.pone.0032505

Editor: Irina Agoulnik, Florida International University, United States of America

Received November 7, 2011; **Accepted** January 31, 2012; **Published** March 30, 2012

Funding: This study was funded by a Programme Hospitalier de Recherch Clinique Inter-Régional (PHRC number UF 8270) provided by CHU de Montpellier and by a grant from Fondation pour la Recherche Médicale FRM110309. The funders had no role in study design, data collection and analysis, decision to publish, or preparation of the manuscript.

Competing Interests: The authors have declared that no competing interests exist.

* E-mail: c-sultan@chu-montpellier.fr

Introduction

The disorders of sex development (DSD) comprise a variety of anomalies defined by congenital conditions in which chromosomal, gonadal, or anatomical sex is atypical. The prevalence of the 46,XY disorders of sex development (46,XY DSD) is difficult to determine with accuracy because of the heterogeneity in the clinical presentation and the etiologies. The estimated incidence of severe 46,XY DSD with uncertain sex is 2.2 per 10,000 births [1], and for a minor form of 46,XY DSD with isolated and non-severe hypospadias, the incidence is estimated at 1 in 250–400 births [2]. Two independent surveillance systems in the United States, the nationwide Birth Defects Monitoring Program (BDMP) and the Metropolitan Atlanta Congenital Defects Program (MACDP), reported a near doubling in the hypospadias rate in comparison with the immediately preceding decades [3]. Although recent studies have questioned this reported rise and provide conflicting data [4,5], the elucidation of the pathophysiology of these genital malformations remains challenging.

The etiologies of 46,XY DSD are usually gonadal dysgenesis (defect in *SRY* and downstream genes such as *SOX9, WT1, NR5A1* [6,7], etc.), defects in androgen biosynthesis and, more frequently, abnormalities in androgen sensitivity. Unfortunately, more than 50% of children with severe 46,XY DSD presenting with uncertain sex do not have a definitive clinical diagnosis [8]. For instance, an *AR* gene defect is identified in less than 10% of the cases [9].

In addition to these well classified causes, a recent candidate gene was identified as critical for the development of male genitalia: the Mastermind-like domain containing 1 (*MAMLD1*) gene (formerly *CXorf6*). This gene was discovered during studies to find the gene responsible for X-linked myotubular myopathy, *MTM1*, which maps to proximal Xq28 [10]: *MAMLD1* was observed to be deleted in patients with both the myopathy and external genital malformations [10,11,12]. Polymorphisms of *MAMLD1* have been reported in patients with isolated hypospadias, the less severe form of 46,XY DSD, but these variants usually

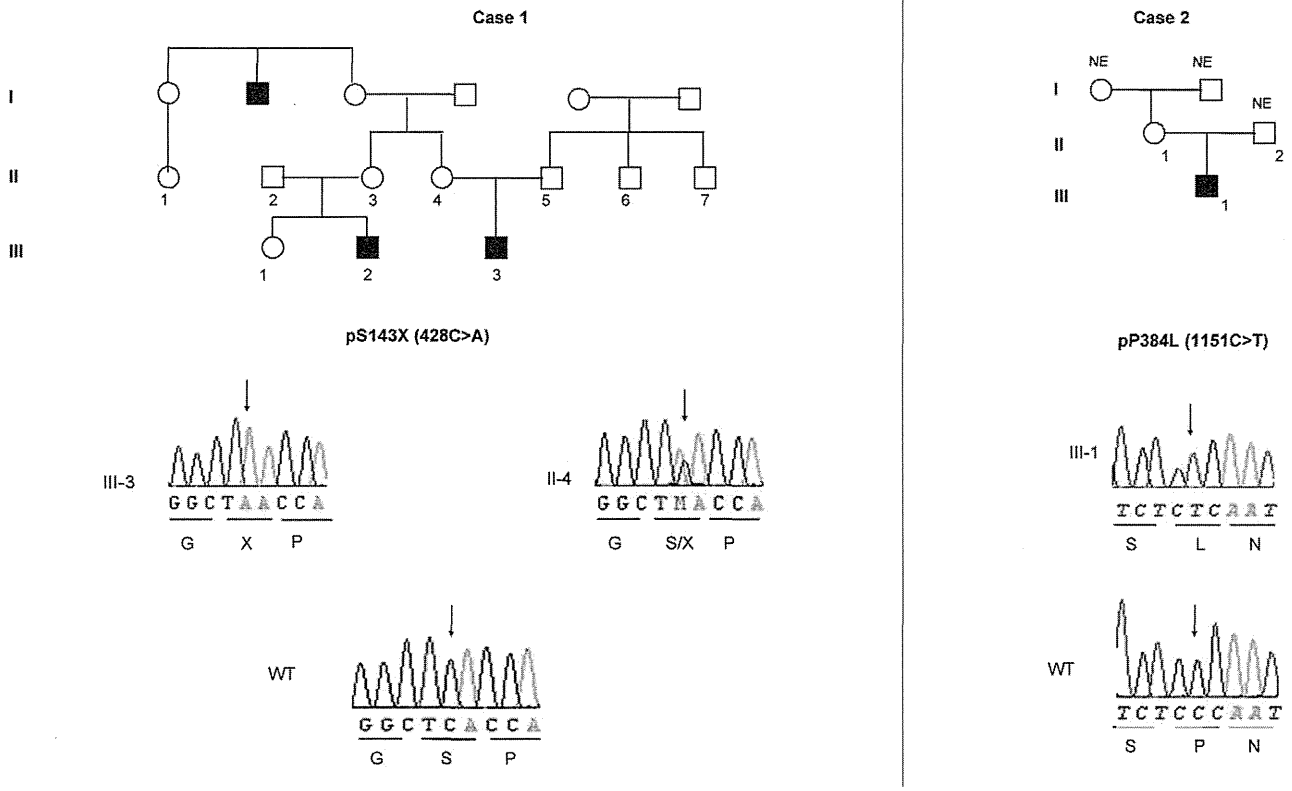

Figure 1. Electrochromatograms and pedigrees of the three patients with *MAMLD1* mutations. The black squares indicate patients with posterior hypospadias. All mutant sequences were controlled by wildtype (WT) DNA. Regarding case 1's family, only the members III-3 and II-4 were genotyped, as the other members in the pedigree declined genetic testing.
doi:10.1371/journal.pone.0032505.g001

do not affect the transactivation of the protein [13,14]. Conversely, severe 46,XY DSD with uncertain sex has been sparsely studied. To date, only one study has focused on these patients: Fukami et al. identified three nonsense mutations in four individuals from a group of 166 patients [15]. The aim of the present study was to determine whether *MAMLD1* is frequently implicated in newborns and children with severe 46,XY DSD with uncertain sex and whether *MAMLD1* should be routinely sequenced in these patients.

Materials and Methods

Patients and controls

Two hundred and twenty individuals were included in this study. Seventy children presented with non-syndromic 46,XY DSD of unknown etiology. According to the Quigley classification [16], 8 patients exhibited a stage 2 phenotype; 32 patients, stage 3; 20 patients, stage 4; 5 patients, stage 5; and 5 patients, stage 6. One hundred and fifty healthy individuals were included as controls. Controls were chosen among patients without urinary, genital, or endocrine disease, or any other congenital malformation. For instance, patients with acute appendicitis or operated on for circumcision without phimosis were included. This study was approved by the Institutional Review Board (CPP-Montpellier, ID RCB No. 2008-A00781-54). Written consent was obtained from the parents, carers or guardians on behalf of the participating minors. When a mutation was identified, other family members were examined if possible. The patients and controls were Caucasian.

DNA extraction

DNA was extracted from peripheral blood using a QIAamp DNA blood minikit (Qiagen, Courtaboeuf, France).

Mutational analysis of MAMLD1

Direct sequencing of *MAMLD1* coding exons and their flanking splice sites was performed in all patients and controls using primers as previously described [17]. The 3730xl DNA Analyzer (Applied Biosystems, Foster City, CA, USA) was used. Sequencing reactions were repeated twice with at least two different PCR products. The DNA sequences were compared with the sequences of normal controls and the reference genomes from the ensembl.org database (Ensembl: ENSG00000013619) and the genebank database (MIM: 300120, NCBI Gene ID: 10046). It is notable that the number of the cDNA and amino acids has been changed recently because of the recognition of a novel *MAMLD1* start codon. This report describes *MAMLD1* cDNA and amino acids according to the new system.

Molecular analysis of androgen sensitivity

A molecular analysis of the androgen receptor (*AR*) and 5 alpha reductase type 2 (*SRD5A2*) genes was performed in all patients.

Table 1. Clinical and hormonal data of patients with mutated *MAMLD1*.

Patient	Case 1	Case 2
MAMLD1 mutation	pS143X	pP384L
Previous medical history	None	Maternal diabetes
Genital phenotype		
Urethral meatus	Scrotal	Penile posterior
Age at exam (yr,mo)	0,0	0,0
Microphallus	Yes, 20 mm	Yes, 20 mm with cuvature
Testis position	Intra-scrotal	Intra-scrotal
Testis size (normal = 1–2 ml)	Normal	Normal
Scrotal appearance	Ventral transposition, Bifid Scrotum	Bifid Scrotum
Renal and urinary tract structure	Normal	Normal
Extragenital phenotype	Normal	Normal
Growth		
Birth height, cm (SDS)	51 (+0)	50.5 (+0)
Birth weight, Kg (SDS)	3.540 (+0)	3.750 (+0.5)
Serum hormone level		
Time of measurment (yr,mo)	0,0	0,3
Testosterone (ng/ml) (1–3 ng/ml)	1.78	<0.07
LH (UI/l) (1–12 UI/l)	10	0.3
FSH (UI/l) (1–10 UI/l)	0.8	0.8
AMH	336 ng/ml	19 ng/ml*
Inhibin	NA	<15 ng/ml*

SD: standard deviation. ND: not determined. NA: not available. DHT: dihydrotestosterone. DHEA: dihydroepiandrsosterone. Parentheses indicate the standard deviation for height and weight and the normal range for hormone serum levels. Testes of 1–2 ml can be regarded as normal, as recently reported by Shibata et al. [34].
*It is notable that anti-mullerian hormone and inhibin were lowered in one case. *MAMLD1* is indeed reported to be expressed in Sertoli cells, as well [15].
doi:10.1371/journal.pone.0032505.t001

Exons 1–8 of the *AR* gene were amplified by PCR using sets of primers and reactions previously described [18]. Molecular analysis of the *SRD5A2* gene (exons 1–5) was performed as previously reported [19]. PCRs were verified for correct length on agarose gel, purified with Qiaquick PCR columns (Qiagen), and sequenced with the ABI Prism Big Dye terminator sequencing kit. *NR5A1*was sequenced in 46,XY DSD children with low plasma testosterone as previously published [6,20].

Homology study

Ensembl.org detected the putative homologs of the human *MAMLD1* gene and alignments were made with the ClustalW software at http://www.ebi.ac.uk/Tools/msa/clustalw2/.

Structure prediction

The potential impact of variants was first predicted using X *in-silico* tools for secondary structure, tertiary structure and prediction of the consequences of amino acid changes.

The secondary structure for wildtype and variants was predicted using JPred software [21] (http://www.compbio.dundee.ac.uk/www-jpred/). The relative accessibility of amino acids was studied with Netsurf software [22] (http://www.cbs.dtu.dk/services/NetSurfP/). The three-dimensional structure was predicted by the Protein Homology/analogY Recognition Engine (PhyreEngine) from the Structural Bioinformatics Group, Imperial College, London, at http:www.sbg.bio.ic.ac.uk/phyrew/. This tool can detect remote homologous proteins with similar tertiary structures, based on multiple sequence profiles with structure-based profiles [23].

The functional consequences of amino acid changes were predicted using four algorithms. Polyphen (Harvard, USA) [24,25], Panther [26], Sift (University of British Columbia) [27] and SNP-3D (University of Maryland) [28] were used, respectively, at http://genetics.bwh.harvard.edu/pph/, http://www.pantherdb.org/tools/csnpScoreForm.jsp., http://sift.jcvi.org/, and http://www.snps3d.org/modules.php?name=Search&op=advanced%20search. These algorithms are based on the alignment of orthologous and/or paralogous protein sequences and/or structural constraints.

Transactivation analysis of MAMLD1

The transactivation function of the variant MAMLD1 proteins was analyzed by the luciferase method [29]. We used the previously reported luciferase reporter vector containing the promoter sequence of mouse hairy/enhancer of split 3 (*Hes3*) (–2,715~+261 bp) [30] and expression vectors containing cDNAs for wildtype *MAMLD1*, p.S143X and p.P384L [29]. Mouse Leydig tumor (MLTC1) cells (ATCC, CRL-2065) seeded in 12-well dishes ($0.5–1.0\times10^5$ cells/well) were transiently transfected using Lipofectamine 2000 (Invitrogen) with 0.6 μg of luciferase reporter vector and 0.6 μg of expression vector for wildtype or variant *MAMLD1*, together with 20 ng of pRL-CMV vector (Promega) used as an internal control. As a control for the expression vectors, an empty counterpart vector was transfected. Luciferase assays performed with a Lumat LB9507 (Berthold) 48 hours after transfection were repeated three times.

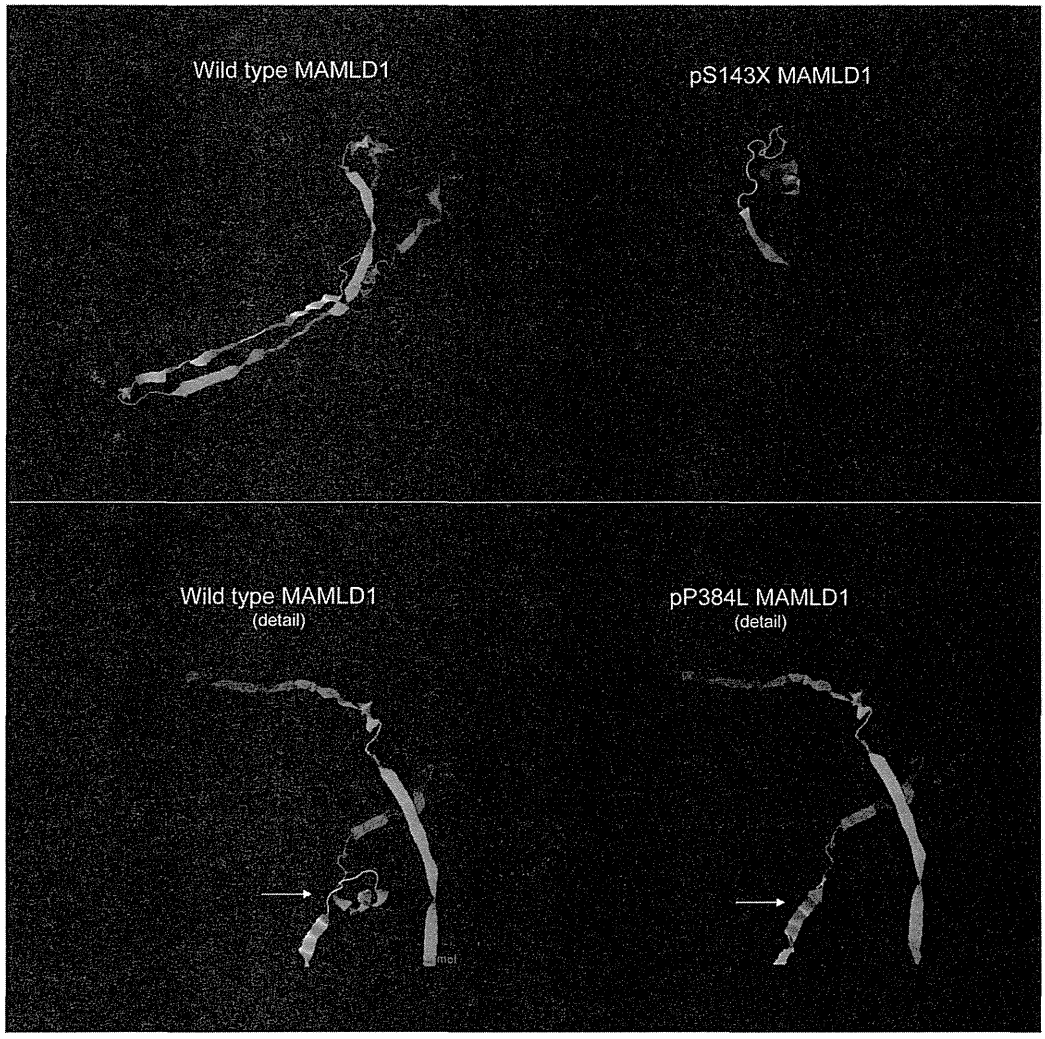

Figure 2. Tertiary structure prediction of the wildtype protein (left column) and with the mutants. 3D structure was predicted at Protein Homology/analogY Recognition Engine (PhyreEngine) from the Structural Bioinformatics Group, Imperial College, London, at http:www.sbg.bio.ic.ac.uk/phyre~/. The plain arrows show the changes in the shape of the protein between the wildtype and p.P384L.
doi:10.1371/journal.pone.0032505.g002

Statistical methods

Haplotype frequencies were compared between cases and controls using the χ^2 test and the Fisher test on SPSS 16.0 software. The odds ratio (OR) was also considered with the logit confidence intervals method: $OR-CI=e^{LN(OR)\pm 1.96\left(\frac{1}{A}+\frac{1}{B}+\frac{1}{C}+\frac{1}{D}\right)^{0.5}}$. Hapmap and ensembl.org were used to exclude linkage disequilibrium. Regarding the transactivation analysis of *MAMLD1*, the results are expressed using the mean and SD, and statistical significance was determined by the *t*-test.

Results

Mutations of MAMLD1 and functional analyses

Among the 70 newborns and children with 46,XY DSD, two new mutations were identified in two unrelated patients: p.S143X (c.428C>A) and p.P384L (c.1151C>T) (Fig. 1). The clinical and genetic data are summarized in Table 1. None of these mutations was noted in the control group. The sequences of the *AR*, *SRD5A2* and *NR5A1* genes were normal in these patients.

a- The p.S143X mutation was predicted to cause a short and truncated protein. The *in silico* prediction showed profoundly modified amino acid accessibility and 3D structure. Relative surface accessibility and absolute surface accessibility of the last amino acid changed from 0.248 to 0.834 and from 29.124 to 97.721, respectively. PhyreEngine predicted the loss of any functional site without a residual consensus sequence (no homologous sequence over 5% through whole genome) (Fig. 2). The *in vitro* functional study confirmed no residual transactivating function of the mutant (Fig. 3). Interestingly, a maternal uncle and a maternal cousin of the index case both exhibited severe hypospadias (not available for genetic testing). The mother was indeed heterozygous for the mutation (Fig. 1).

b- The p.P384L mutation was found in a patient with posterior penile hypospadias and microphallus. No cryptrochidism was noted. The secondary structure was predicted to be changed in the next four amino acids. The relative and absolute accessibilities of the amino acid were modified from 0.27 to 0.35 and from 39.07 to 65.25, respectively. The 3D structure prediction of the mutated protein was significantly changed (Fig. 2). All four *in silico*

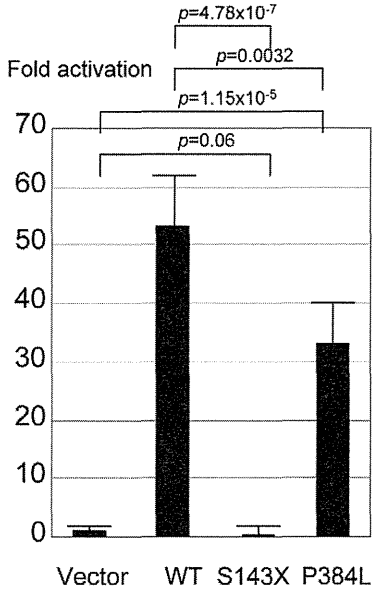

Figure 3. Transactivation function of the variants of the MAMLD1 protein analyzed by the luciferase method. The activity is evaluated for pHes3-luc vector.
doi:10.1371/journal.pone.0032505.g003

algorithms predicted affected protein function (Table 2) with a conserved amino acid throughout species (Table 3). Functional studies confirmed the significantly reduced transactivation function of the p.P384L protein with 60% residual activity when compared with the wildtype protein, $p = 0.0032$ (Fig. 3).

Polymorphisms of MAMLD1

We identified three polymorphisms of *MAMLD1* in our series: p.P359S (c.1075C>T, rs41313406), p.N662S (c.1985A>G, rs2073043) and p.H347Q (c.1041C>A, rs62641609). Regarding the p.P359S and p.N662S polymorphisms, 14 patients exhibited double polymorphisms (S-S haplotype) and five had the p.N359S polymorphism. The phenotypes of the patients with the S-S haplotype were as follows: penile posterior hypospadias and cryptorchidism in three cases, hypospadias and microphallus in five cases (anterior n = 1, penile posterior n = 2 and scrotal hypospadias n = 2), and cryptorchidism and microphallus in six cases (bilateral cryptorchidism n = 5, unilateral cryptorchidism n = 1). Using hapmap and ensembl.org, no linkage disequilibrium was found for these two variants. In previous studies, we and others found that the S-S haplotype was present in only 6/150 controls (4.0%) and 23/360 controls (6.4%) [13,14]. By combining the published series for controls (matched patients and controls), we determined that the incidence of the S-S haplotype was higher in the DSD patients (20%, n = 70 vs. 6%, n = 510, $p = 0.0003$) (OR = 3.86, CI from 1.94 to 7.70, $p = 0.05$). Haplotypes and their relative frequencies in each group of patients are summarized in Table 4.

The p.H347Q variant, previously reported as a polymorphism especially in sub-Saharan populations (rs62641609, http://www.ensembl.org/Homo_sapiens/Variation/Summary?r=X:149638386-149639386;v=rs62641609;vdb=variation;vf=16740729), was identified in a patient with posterior hypospadias and microphallus (25 mm length at birth).

Table 2. Prediction of affected protein function using four algorithms.

Algorithm	pP384L
Polyphen	Probably damaging
	score = 0.961 (sensitivity: 0.71; specificity: 0.93)
Sift	Affect protein function
	Sift score = 0.04
Panther	Probability of deleterious effect = 0.42
	(subPSEC score = −2.7)
SNPS3D	Deleterious
	(svm score = −1.75)

References and online access are indicated in the text. Mathematical calculation of the significance of each score is available online.
doi:10.1371/journal.pone.0032505.t002

Discussion

MAMLD1 is a good candidate to explore in patients with unexplained 46,XY DSD, as it has been shown to be expressed in fetal Leydig cells around the critical period for sex development [15]. The transient knockdown of *MAMLD1* mRNA expression results in significantly reduced testosterone production in mouse Leydig tumor cells [29]. *MAMLD1* is further coexpressed with steroidogenic factor (*NR5A1*), which regulates the transcription of genes involved in sex development, and an *NR5A1*target site was found within the *MAMLD1* gene [29,31]. *MAMLD1* thus seems to have an important role in modulating testosterone production during sex development and is involved in the 46,XY disorders of sex development [32].

Regarding the minor forms of 46,XY DSD with isolated and non-severe hypospadias, mutational studies of *MAMLD1* have identified several polymorphisms in this gene. We reported the following variants in patients with isolated hypospadias: p.P359S, p.V505A, p.N662S and p.604ins3Q [13,17], all of which were recently confirmed as polymorphisms [14]. The p.Q602K mutation was also found in one patient with posterior hypospadias and was predicted to affect the splicing process. An association between isolated hypospadias and the rare haplotype p.P359S-p.N662S is also suspected [13,14].

Table 3. Homology study showed that this amino acid was highly conserved through species for the c.1041C>A and c.1151C>T mutations.

Patient	MSSNTLSGSTLRGS**L**NALLSSMTSSSNAAL
Human-MAMLD1	MSSNTLSGSTLRGS**P**NALLSSMTSSSNAAL
Pig	MSSSSLPGSTLHGS**P**GALLSSGAPSSSSAL
Horse	MSSSNLPGSTLQGS**P**NALLSSMVSGSSAAL
Chimpanzee	MSSNTLSGSTLRGS**P**NALLSSMTSSSNAAL
Mouse	MSSSSLSGSAVQSS**P**NALLSSMAPSSNASL
Rabbit	MAPHSLPGSSLQGS**P**NALLSSMAPNSSGAL
Dog	MASSNLPGSSFQAS**P**NALLASMASASSAGL
Cat	MASGNLPGSAFQGS**P**NALLASMASGSSAAL

doi:10.1371/journal.pone.0032505.t003

Table 4. Incidence of exonic polymorphisms p.P359S and p.N662S, and relative haplotypes in normal controls and 46,XY DSD patients.

Haplotype 359–662	Patients, n = 70	Controls, n = 510	Fisher, p value	OR	OR confidence interval (p = 0.05)
p.359C- p.662A	72.9% (n = 51)	90.6% (n = 462)	p = 0.0001	0.28	0.15–0.51
p.359T- p.662A	0%	1.5% (n = 8)	p = 0.60	0.42	0.02–7.35
p.359C- p.662G	7.1% (n = 5)	0.8% (n = 9)	p = 0.02	4.28	1.39–13.17
p.359T- p.662G (S-S polymorphism)	20% (n = 14)	6% (n = 31)	p = 0.0003	3.86	1.94–7.70

Controls are combined with the published series (matched for ethnicity of patients and controls) [13] [14]. The χ-square test was performed. When combining all patients with the p.662G polymorphism whatever the p.359 allele, this p.662G was significantly more frequent in 46,XY DSD patients: 27.1% (n = 19) vs. 6.8% (n = 40), $p = 0.0001$.

doi:10.1371/journal.pone.0032505.t004

Regarding severe 46,XY DSD with uncertain sex, only one published paper to date has reported three *MAMLD1* mutations (p.E124X, p.Q197X and p.R653X) [15]. It is precisely in this situation of severe genital malformation that the diagnosis of the causative mechanism is of clinical interest for medical treatment (hormone substitution, pubertal follow-up). In order to determine whether this report was an exceptional observation or of practical clinical interest, we screened 70 patients with severe 46,XY DSD of unknown origin. We identified two new mutations of *MAMLD1* in patients with severe hypospadias and microphallus (1 stop codon and 1 missense mutation). These mutations were associated with a severe phenotype, and reduced (p.P384L) or abolished (p.S143X) transactivation function was found in two cases. 46,XY DSD with normal *AR, SRD5A2* and *NR5A1*gene sequences can thus reveal a mutation of *MAMLD1*. This finding suggests a new diagnostic investigation for these patients and may be helpful in genetic counselling if a mutation is identified. It also provides new insight into the pathophysiology of DSD. Indeed, in the family of the child bearing the p.S143X mutation, the mother was heterozygous and two other males on the maternal side of the family exhibited a consistent phenotype. Unfortunately, the family declined any further investigation.

The mechanisms by which these mutations with reduced transactivation induce DSD are still under investigation. As noted above, several studies have provided strong evidence of *MAMLD1* implication in fetal sex development through modulation of testosterone production at the time of sex differentiation. The plasma testosterone measured in one of our cases was indeed lowered but it was normal in the other one, as previously reported in patients with nonsense mutations [15]. Plasma testosterone evaluation is thus not systematically helpful in orienting the diagnosis of DSD since mutations of the genes implicated in testosterone production - such as *MAMLD1* and *NR5A1* - have been reported in 46,XY DSD patients with normal plasma testosterone. These findings, along with the absence of correlation between the *in vitro* functional analysis and the biological and clinical phenotype, suggest that the genital malformation is primarily related to a transient prenatal testicular (Leydig cell) dysfunction and the resulting compromised testosterone production around the critical period of sex differentiation [33]. In the postnatal period, the mouse homolog of *MAMLD1* was indeed reported to be weakly expressed in the testis at one week of age and the expression was faint thereafter.

We also report a high incidence of the rare haplotype p.P359S-p.N662S in our series. The p.P359S (which was designated p.P286S in the previous report) variant was first reported in a patient with hypospadias but it was absent in his brother and nephew with the same phenotype [15]. The p.N662S (which was designated p.P589S in the previous report) variant was found in hypospadiac patients but was also reported in a normal population, although with low incidence [15]. We and others have found that the S-S haplotype is associated with a minor form of DSD, i.e., isolated hypospadias [14], but the *in vitro* functional study of the p.P359S-p.N662S *MAMLD1* variant was inconclusive with unchanged transactivation function [13]. In the present study, we show that the combination of these alleles was present in as much as 15% of patients with severe 46,XY DSD. This is significantly higher than in the controls [combining the series, 15% (n = 70) vs. 10.7% (n = 510), $p = 0.0003$]. Again, a transient testosterone production failure during prenatal development may have contributed to the undervirilization of the external genitalia, but how this haplotype can be present in normal, mild and severe phenotypes remains to be elucidated.

Severe undervirilization in XY newborns can reveal mutations of *MAMLD1*. *MAMLD1* should be routinely sequenced in these patients with otherwise normal *AR, SRD5A2* and *NR5A1* genes.

Acknowledgments

We would like to thank Dr Béroud (Laboratoire de Génétique Chromosomique, Institut Universitaire de Recherche Clinique, Université de Montpellier 1, France) for his great help in the statistical study of haplotypes.

Author Contributions

Conceived and designed the experiments: NK MF CS TO PP. Performed the experiments: NK MF PP FA. Analyzed the data: NK MF PP FA CP JW GP SM MP. Contributed reagents/materials/analysis tools: CP JW GP SM MP. Wrote the paper: NK TO CS PP FA.

References

1. Thyen U, Lanz K, Holterhus PM, Hiort O (2006) Epidemiology and initial management of ambiguous genitalia at birth in Germany. Horm Res 66: 195–203.
2. Nelson P (2007) Epidemiology of Hypospadias. Dialogues in Pediatric Urology 28: 2–3.
3. Paulozzi LJ, Erickson JD, Jackson RJ (1997) Hypospadias trends in two US surveillance systems. Pediatrics 100: 831–834.
4. Martinez-Frias ML, Prieto D, Prieto L, Bermejo E, Rodriguez-Pinilla E, et al. (2004) Secular decreasing trend of the frequency of hypospadias among newborn male infants in Spain. Birth Defects Res A Clin Mol Teratol 70: 75–81.
5. Fisch H, Hyun G, Hensle TW (2010) Rising hypospadias rates: disproving a myth. J Pediatr Urol 6: 37–39.
6. Lin L, Philibert P, Ferraz-de-Souza B, Kelberman D, Homfray T, et al. (2007) Heterozygous missense mutations in steroidogenic factor 1 (SF1/Ad4BP,

NR5A1) are associated with 46,XY disorders of sex development with normal adrenal function. J Clin Endocrinol Metab 92: 991–999.
7. Coutant R, Mallet D, Lahlou N, Bouhours-Nouet N, Guichet A, et al. (2007) Heterozygous mutation of steroidogenic factor-1 in 46,XY subjects may mimic partial androgen insensitivity syndrome. J Clin Endocrinol Metab 92: 2868–2873.
8. Morel Y, Rey R, Teinturier C, Nicolino M, Michel-Calemard L, et al. (2002) Aetiological diagnosis of male sex ambiguity: a collaborative study. Eur J Pediatr 161: 49–59.
9. Choi J, Kim G, Seo E, KS K, Kim S, et al. (2008) Molecular analysis of the AR and SRD5A2 genes in patients with 46,XY disorders of sex development. J Pediatr Endocrinol Metab 21: 545–553.
10. Laporte J, Kioschis P, Hu LJ, Kretz C, Carlsson B, et al. (1997) Cloning and characterization of an alternatively spliced gene in proximal Xq28 deleted in two patients with intersexual genitalia and myotubular myopathy. Genomics 41: 458–462.
11. Bartsch O, Kress W, Wagner A, Seemanova E (1999) The novel contiguous gene syndrome of myotubular myopathy (MTM1), male hypogenitalism and deletion in Xq28:report of the first familial case. Cytogenet Cell Genet 85: 310–314.
12. Hu LJ, Laporte J, Kress W, Kioschis P, Siebenhaar R, et al. (1996) Deletions in Xq28 in two boys with myotubular myopathy and abnormal genital development define a new contiguous gene syndrome in a 430 kb region. Hum Mol Genet 5: 139–143.
13. Kalfa N, Cassorla F, Audran F, Oulad Abdennabi I, Philibert P, et al. (2011) Polymorphisms of MAMLD1 gene in hypospadias. J Pediatr Urol 7: 585–591.
14. Chen Y, Thai HT, Lundin J, Lagerstedt-Robinson K, Zhao S, et al. (2010) Mutational study of the MAMLD1-gene in hypospadias. Eur J Med Genet 53: 122–126.
15. Fukami M, Wada Y, Miyabayashi K, Nishino I, Hasegawa T, et al. (2006) CXorf6 is a causative gene for hypospadias. Nat Genet 38: 1369–1371.
16. Quigley CA, French FS (1994) Androgen insensitivity syndromes. Curr Ther Endocrinol Metab 5: 342–351.
17. Kalfa N, Liu B, Ophir K, Audran F, Wang MH, et al. (2008) Mutations of CXorf6 are associated with a range of severities of hypospadias. Eur J Endocrinol 159: 453–458.
18. Philibert P, Audran F, Pienkowski C, Morange I, Kohler B, et al. (2010) Complete androgen insensitivity syndrome is frequently due to premature stop codons in exon 1 of the androgen receptor gene: an international collaborative report of 13 new mutations. Fertil Steril 94: 472–476.
19. Maimoun L, Philibert P, Cammas B, Audran F, Bouchard P, et al. (2010) Phenotypical, Biological, and Molecular Heterogeneity of 5{alpha}-Reductase Deficiency: An Extensive International Experience of 55 Patients. J Clin Endocrinol Metab 96: 296–307.
20. Philibert P, Leprieur E, Zenaty D, Thibaud E, Polak M, et al. (2010) Steroidogenic factor-1 (SF-1) gene mutation as a frequent cause of primary amenorrhea in 46,XY female adolescents with low testosterone concentration. Reprod Biol Endocrinol 8: 28.
21. Cole C, Barber JD, Barton GJ (2008) The Jpred 3 secondary structure prediction server. Nucleic Acids Res 36: W197–201.
22. Petersen B, Petersen TN, Andersen P, Nielsen M, Lundegaard C (2009) A generic method for assignment of reliability scores applied to solvent accessibility predictions. BMC Struct Biol 9: 51.
23. Kelley LA, Sternberg MJ (2009) Protein structure prediction on the Web: a case study using the Phyre server. Nat Protoc 4: 363–371.
24. Ramensky V, Bork P, Sunyaev S (2002) Human non-synonymous SNPs: server and survey. Nucleic Acids Res 30: 3894–3900.
25. Thomas PD, Kejariwal A (2004) Coding single-nucleotide polymorphisms associated with complex vs. Mendelian disease: evolutionary evidence for differences in molecular effects. Proc Natl Acad Sci U S A 101: 15398–15403.
26. Mi H, Dong Q, Muruganujan A, Gaudet P, Lewis S, et al. (2010) PANTHER version 7: improved phylogenetic trees, orthologs and collaboration with the Gene Ontology Consortium. Nucleic Acids Res 38: D204–210.
27. Kumar P, Henikoff S, Ng PC (2009) Predicting the effects of coding non-synonymous variants on protein function using the SIFT algorithm. Nat Protoc 4: 1073–1081.
28. Yue P, Melamud E, Moult J (2006) SNPs3D: candidate gene and SNP selection for association studies. BMC Bioinformatics 7: 166.
29. Fukami M, Wada Y, Okada M, Kato F, Katsumata N, et al. (2008) Mastermind-like domain containing 1 (MAMLD1 or CXorf6) transactivates the Hes3 promoter, augments testosterone production, and contains the SF1 target sequence. J Biol Chem 29: 5525–5532.
30. Nishimura M, Isaka F, Ishibashi M, Tomita K, Tsuda H, et al. (1998) Structure, chromosomal locus, and promoter of mouse Hes2 gene, a homologue of Drosophila hairy and Enhancer of split. Genomics 49: 69–75.
31. Sadovsky Y, Dorn C (2000) Function of steroidogenic factor 1 during development and differentiation of the reproductive system. Rev Reprod 5: 136–142.
32. Ogata T, Laporte J, Fukami M (2009) MAMLD1 (CXorf6): a new gene involved in hypospadias. Horm Res 71: 245–252.
33. Welsh M, MacLeod DJ, Walker M, Smith LB, Sharpe RM (2010) Critical androgen-sensitive periods of rat penis and clitoris development. Int J Androl 33: e144–152.
34. Shibata Y, Kojima Y, Mizuno K, Nakane A, Kato T, et al. Optimal cutoff value of contralateral testicular size for prediction of absent testis in Japanese boys with nonpalpable testis. Urology 76: 78–81.

Epigenetics 7:10, 1142–1150; October 2012; © 2012 Landes Bioscience

Paternal uniparental disomy 14 and related disorders

Placental gene expression analyses and histological examinations

Masayo Kagami,[1] Kentaro Matsuoka,[2] Toshiro Nagai,[3] Michiko Yamanaka,[4] Kenji Kurosawa,[5] Nobuhiro Suzumori,[6] Yoichi Sekita,[7] Mami Miyado,[1] Keiko Matsubara,[1] Tomoko Fuke,[1] Fumiko Kato,[1,8] Maki Fukami[1] and Tsutomu Ogata[1,8,*]

[1]Department of Molecular Endocrinology; National Research Institute for Child Health and Development; Tokyo, Japan; [2]Departments of Pathology; National Center for Child Health and Development; Tokyo, Japan; [3]Department of Pediatrics; Dokkyo University School of Medicine; Koshigaya, Japan; [4]Department of Integrated Women's Health; St. Luke's International Hospital; Tokyo, Japan; [5]Division of Medical Genetics; Kanagawa Children's Medical Center; Yokohama, Japan; [6]Department of Obstetrics and Gynecology; Nagoya City University Graduate School of Medicine; Nagoya, Japan; [7]Department of Pathology; Graduate School of Medicine; Osaka University, Osaka, Japan; [8]Department of Pediatrics; Hamamatsu University School of Medicine; Hamamatsu, Japan

Keywords: Upd(14)pat, microdeletion, placenta, expression dosage, histopathology, imprinting

Abbreviations: *PEGs*, paternally expressed genes; *MEGs*, maternally expressed genes; DMRs, differentially methylated regions; IG-DMR, *DLK1-MEG3* intergenic DMR; *RTL1as*, *RTL1* antisense; upd(14)pat, paternal uniparental disomy 14; BWS, Beckwith-Wiedemann syndrome; q-PCR, quantitative real-time PCR; CGH, oligoarray comparative genomic hybridization; LM, light microscopic; EM, electron microscopic; IHC, immunohistochemical

Although recent studies in patients with paternal uniparental disomy 14 [upd(14)pat] and other conditions affecting the chromosome 14q32.2 imprinted region have successfully identified underlying epigenetic factors involved in the development of upd(14)pat phenotype, several matters, including regulatory mechanism(s) for *RTL1* expression, imprinting status of *DIO3* and placental histological characteristics, remain to be elucidated. We therefore performed molecular studies using fresh placental samples from two patients with upd(14)pat. We observed that *RTL1* expression level was about five times higher in the placental samples of the two patients than in control placental samples, whereas *DIO3* expression level was similar between the placental samples of the two patients and the control placental samples. We next performed histological studies using the above fresh placental samples and formalin-fixed and paraffin-embedded placental samples obtained from a patient with a maternally derived microdeletion involving *DLK1*, the IG-DMR, the *MEG3*-DMR and *MEG3*. Terminal villi were associated with swollen vascular endothelial cells and hypertrophic pericytes, together with narrowed capillary lumens. DLK1, RTL1 and DIO3 proteins were specifically identified in vascular endothelial cells and pericytes, and the degree of protein staining was well correlated with the expression dosage of corresponding genes. These results suggest that *RTL1as*-encoded microRNA functions as a repressor of *RTL1* expression, and argue against *DIO3* being a paternally expressed gene. Furthermore, it is inferred that DLK1, DIO3 and, specially, RTL1 proteins, play a pivotal role in the development of vascular endothelial cells and pericytes.

Introduction

Human chromosome 14q32.2 region carries a cluster of imprinted genes including protein coding paternally expressed genes (*PEGs*) such as *DLK1* and *RTL1* (alias *PEG11*) and non-coding maternally expressed genes (*MEGs*) such as *MEG3* (alias *GTL2*) and *RTL1as* (*RTL1* antisense encoding microRNAs).[1,2] The 14q32.2 imprinted region also harbors two differentially methylated regions (DMRs), i.e., the germline-derived primary *DLK1-MEG3* intergenic DMR (IG-DMR) and the postfertilization-derived secondary *MEG3*-DMR.[1,2] Both DMRs are hypermethylated after paternal transmission and hypomethylated after maternal transmission in the body, whereas in the placenta the IG-DMR alone remains as a DMR and the *MEG3*-DMR is rather hypomethylated.[2] We have previously revealed that the hypomethylated IG-DMR and *MEG3*-DMR of maternal origin function as imprinting control centers in the placenta and the body, respectively, and that the IG-DMR functions hierarchically as an upstream regulator for the methylation pattern of the *MEG3*-DMR on the maternally inherited chromosome in the body, but not in the placenta.[3]

*Correspondence to: Tsutomu Ogata; Email: tomogata@hama-med.ac.jp
Submitted: 06/21/12; Revised: 08/20/12; Accepted: 08/22/12
http://dx.doi.org/10.4161/epi.21937

Consistent with these findings, paternal uniparental disomy 14 [upd(14)pat] results in a unique phenotype characterized by facial abnormality, small bell-shaped thorax with coat hanger appearance of the ribs, abdominal wall defects, placentomegaly and polyhydramnios.[2,4] We have studied multiple patients with upd(14)pat and related conditions, such as epimutations of the maternally derived DMRs and various types of microdeletions involving the maternally inherited imprinted region, suggesting that markedly increased *RTL1* expression is the major underlying factor for the development of upd(14)pat-like phenotype.[2] The notion of excessive *RTL1* expression is primarily based on the following mouse data indicating a trans-acting repressor function of *Rtl1as*-encoded microRNAs for *Rtl1* expression: (1) targeted deletion of the maternally derived IG-DMR causes maternal to paternal epigenotypic switch of the imprinted region, with ~4.5 times rather than ~2 times of *Rtl1* expression as well as ~2 times of *Dlk1* expression and nearly absent *Megs* expression, in the presence of two functional copies of *Pegs* and no functional copy of *Megs*[5] and; (2) targeted deletion of the maternally derived *Rtl1as* results in 2.5–3.0 times of *Rtl1* expression, in the presence of a single functional copy of *Rtl1*.[6] Similarly, in the human, typical upd(14)pat phenotype is observed in patients with epimutations that are likely associated with markedly increased *RTL1* expression because of the combination of two functional copies of *RTL1* and no functional copy of *RTL1as*, whereas relatively mild upd(14)pat-like phenotype is found in patients with maternally inherited microdeletions involving *RTL1as* that are likely accompanied by moderately elevated *RTL1* expression because of the combination of a single functional copy of *RTL1* and no functional copy of *RTL1as*.[2]

Human imprinting disorders are usually associated with placental abnormalities. For example, Beckwith-Wiedemann syndrome (BWS) and upd(14)pat are associated with placentomegaly,[4,7] and Silver-Russell syndrome is accompanied by hypoplastic placenta.[8] Similarly, mouse imprinting aberrations also usually affect placental growth and development.[9] In agreement with this, virtually all the imprinted genes studied to date are expressed in the placenta and play a pivotal role in the placental growth and development,[10] although placental structure is more or less different between placental animals.[11]

However, several matters remain to be clarified in upd(14)pat and related conditions. For example, it is unknown whether human *RTL1* expression is actually elevated in the absence of functional *RTL1as*-encoded microRNAs. It is also unknown whether *DIO3* is a *PEG*, although mouse *Dio3* has been shown to undergo partial imprinting.[12] In this regard, while we examined fresh blood cells, cultured skin fibroblasts and formalin-fixed and paraffin-embedded placental and body samples obtained from patients with upd(14)pat-like phenotype, precise assessment of *RTL1* and *DIO3* expression levels was impossible because of extremely low *RTL1* and *DIO3* expression levels in fresh blood cells and cultured skin fibroblasts and poor quality of RNAs extracted from paraffin-embedded tissues.[2,3] In addition, while cSNP genotyping has demonstrated paternal *DLK1* and *RTL1* expression and maternal *MEG3* expression in the body and the placenta,[2,3] no informative cSNP data showing paternal *DIO3* expression have been obtained.[2,3] Furthermore, although standard light microscopic (LM) examinations have been performed using formalin-fixed and paraffin-embedded placental samples, fine placental histopathological studies, such as electron microscopic (EM) examinations and immunohistochemical (IHC) examinations, remain to be performed.

To examine these unresolved matters, fresh placental tissues are highly useful, because precise quantitative real-time PCR (q-PCR) analyses and EM studies can be performed with fresh placentas. Thus, we performed q-PCR analyses and EM studies, as well as IHC studies with RTL1 antibodies produced by ourselves and commercially available DLK1 and DIO3 antibodies, using fresh placental samples obtained from two previously reported patients with prenatally diagnosed upd(14)pat.[13,14] We also performed IHC studies using formalin-fixed and paraffin-embedded placental samples obtained from a previously reported patient with a microdeletion involving *DLK1*, but not *RTL1* and *DIO3*,[2] to compare the placental protein expression levels between upd(14)pat and the microdeletion. Furthermore, we also studied a hitherto unreported patient with an unbalanced translocation involving the 14q32.2 imprinted region, to obtain additional data regarding the *RTL1-RTL1as* interaction and the primary factor for the development of upd(14)pat phenotype.

Results

Patients and samples. This study consisted of three previously reported patients with typical body and placental upd(14)pat phenotype and a normal karyotype (cases 1–3),[2,13-15] and a new patient with various non-specific features and a 46,XX,der(17)t(14;17)(q31;p13) karyotype accompanied by three copies of the distal 14q region and a single copy of the terminal 17p region (case 4) . Clinical phenotypes of cases 1–4 are summarized in **Table S1**. In brief, cases 1 and 2 were suspected to have upd(14)pat phenotype including bell-shaped thorax by prenatal ultrasound studies performed for polyhydroamnios, and were confirmed to have upd(14)pat by microsatellite analysis after birth. Case 3 was found to have typical upd(14)pat phenotype during infancy and was shown to have a maternally derived microdeletion affecting the chromosome 14q32.2 imprinted region. Case 4 had growth failure, developmental delay, multiple non-specific anomalies, and omphalocele. There was no history of polyhydramnios or placentomegaly. Thus, except for omphalocele, case 4 had no upd(14)pat-like phenotype. The parental karyotype was normal, indicating a de novo occurrence of the unbalanced translocation.

We obtained fresh placental samples immediately after birth from prenatally diagnosed cases 1 and 2 for molecular studies using genomic DNA and RNA, and fresh leukocyte samples from cases 1, 2 and 4 and their parents for molecular studies using genomic DNA. The fresh placental samples of cases 1 and 2 were also utilized for histopathological examinations, together with formalin-fixed and paraffin-embedded placental samples of case 3. For controls, we obtained three fresh placentas at 37 weeks of gestation, and fresh leukocytes from three adult subjects; for molecular studies using placentas, we prepared pooled samples

consisting of an equal amount of DNA or RNA extracted from each placenta.

Molecular studies in cases 1 and 2. We performed microsatellite analysis for 19 loci on chromosome 14 and bisulfite sequencing for the IG-DMR (CG4 and CG6) and the *MEG3*-DMR (CG7), using placental and leukocyte genomic DNA samples; while microsatellite analysis had been performed for 15 loci in case 1 and 16 loci in case 2, only leukocyte genomic DNA samples were examined in the previous study.[15] Consequently, we identified two peaks for *D14S609* and single peaks for the remaining loci in case 1 (the combination of paternal heterodisomy and isodisomy), and single peaks for all the examined loci in case 2 (apparently full paternal isodisomy) (**Table S2**). Furthermore, no trace of maternally inherited peak was identified in both placental and leukocyte genomic DNA samples (**Fig. 1**). Bisulfite sequencing showed that both the IG-DMR and the *MEG3*-DMR were markedly hypermethylated in the leukocytes of cases 1 and 2, whereas in the placental samples the IG-DMR was obviously hypermethylated and the *MEG3*-DMR was grossly hypomethylated to an extent similar to that identified in control placentas (**Fig. 2**). Furthermore, q-PCR analysis for placental RNA samples revealed that *DLK1*, *RTL1*, and *DIO3* expression levels were 3.3 times, 6.1 times and 1.9 times higher in the placental samples of case 1 than in the control placental samples, respectively, and were 3.1 times, 9.4 times and 1.7 times higher in the placental samples of case 2 than in the control placental samples, respectively (**Fig. 3A**). By contrast, the expressions of all *MEGs* examined were virtually absent in the placental samples of cases 1 and 2. PCR products were sufficiently obtained after 30 cycles for the fresh placental as well as leukocyte samples, consistent with high quality of DNA and RNA obtained from fresh materials.

Molecular studies in case 3. Detailed molecular findings have already been reported previously.[2] In brief, microsatellite analysis revealed biparentally derived homologs of chromosome 14, and a deletion analysis demonstrated a maternally inherited 108,768 bp microdeletion involving *DLK1*, the IG-DMR, the *MEG3*-DMR, and *MEG3*, but not affecting *RTL1/RTL1as*. Since loss of the DMRs causes maternal to paternal epigenotypic alteration,[2] it is predicted that case 3 has a single functional copy of *DLK1* and two functional copies of *RTL1* and *DIO3*, as well as no functional copy of *RTL1as* and other *MEGs*. Bisulfite sequencing showed that both the IG-DMR and the *MEG3*-DMR were markedly hypermethylated in leukocytes, whereas in the formalin-fixed and paraffin-embedded placental samples the IG-DMR was obviously hypermethylated and the *MEG3*-DMR was comprised of roughly two-thirds of hypermethylated clones and roughly one-third of hypomethylated clones. In addition, RT-PCR analysis for such placental samples indicated positive *PEGs* (especially *RTL1*) expression and absent *MEGs* expression. For the formalin-fixed and paraffin-embedded placental samples, PCR products could be obtained only after 35 cycles, because of poor quality (severe degradation) of DNA and RNA.

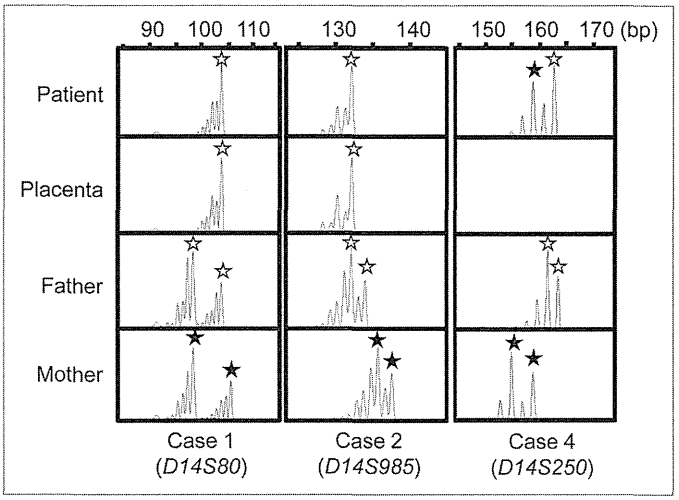

Figure 1. Representative results of microsatellite analysis, using leukocyte genomic DNA samples of the patient and the parents and placental genomic DNA samples. In cases 1 and 2, one of the two paternal peaks is inherited by the patients and the placentas, and no trace of maternal peaks is identified. In case 4, both paternally and maternally derived peaks are found in the patient, with the paternally derived long peak being larger than the maternally inherited short peak.

Molecular findings in case 4. We examined the presence or absence of the 14q32.2 imprinted region on the der(17) chromosome (**Fig. 4**). Oligoarray comparative genomic hybridization (CGH) indicated three copies of a ~19.6 Mb 14q31–qter region, and FISH analysis for four segments around the chromosome 14q32.2 imprinted region delineated positive signals on the der(17) chromosome as well as on the normal chromosome 14 homologs. This demonstrated the presence of the 14q32.2 imprinted region on the der(17) chromosome. In addition, similar oligoarray CGH and FISH analysis revealed loss of a ~455 kb region from the distal chromosome 17p (**Fig. S1**).

Thus, we investigated the parental origin of the translocated 14q distal region. Microsatellite analysis for *D14S250* and *D14S1007* on the translocated 14q distal region delineated biparentally derived two peaks, with paternally derived long PCR products showing larger peaks than maternally derived short PCR products (**Fig. 1**; **Table S2**). Since short products are usually more easily amplified than long products, this indicated paternal

Figure 2 (See opposite page). Bisulfite sequencing analysis of the IG-DMR (CG4 and CG6) and the *MEG3*-DMR (CG7), using leukocyte and placental genomic DNA samples. Filled and open circles indicate methylated and unmethylated cytosines at the CpG dinucleotides, respectively. Upper part: structure of CG4, CG6, and CG7. Pat, paternally derived chromosome; Mat, maternally derived chromosome. The PCR products for CG4 (311 bp) harbor 6 CpG dinucleotides and a G/A SNP (*rs12437020*), those for CG6 (428 bp) carry 19 CpG dinucleotides and a C/T SNP (*rs10133627*) and those for CG7 (168 bp) harbor 7 CpG dinucleotides. Lower part: the results of cases 1, 2, 4 and a control subject. Each horizontal line indicates a single subcloned allele. The control data represent the methylation patterns obtained with a leukocyte genomic DNA sample extracted from a single subject heterozygous for the G/A SNP (*rs12437020*) (body) and those obtained with a pooled DNA sample consisting of an equal amount of genomic DNA extracted from three control placentas homozygous for that SNP.

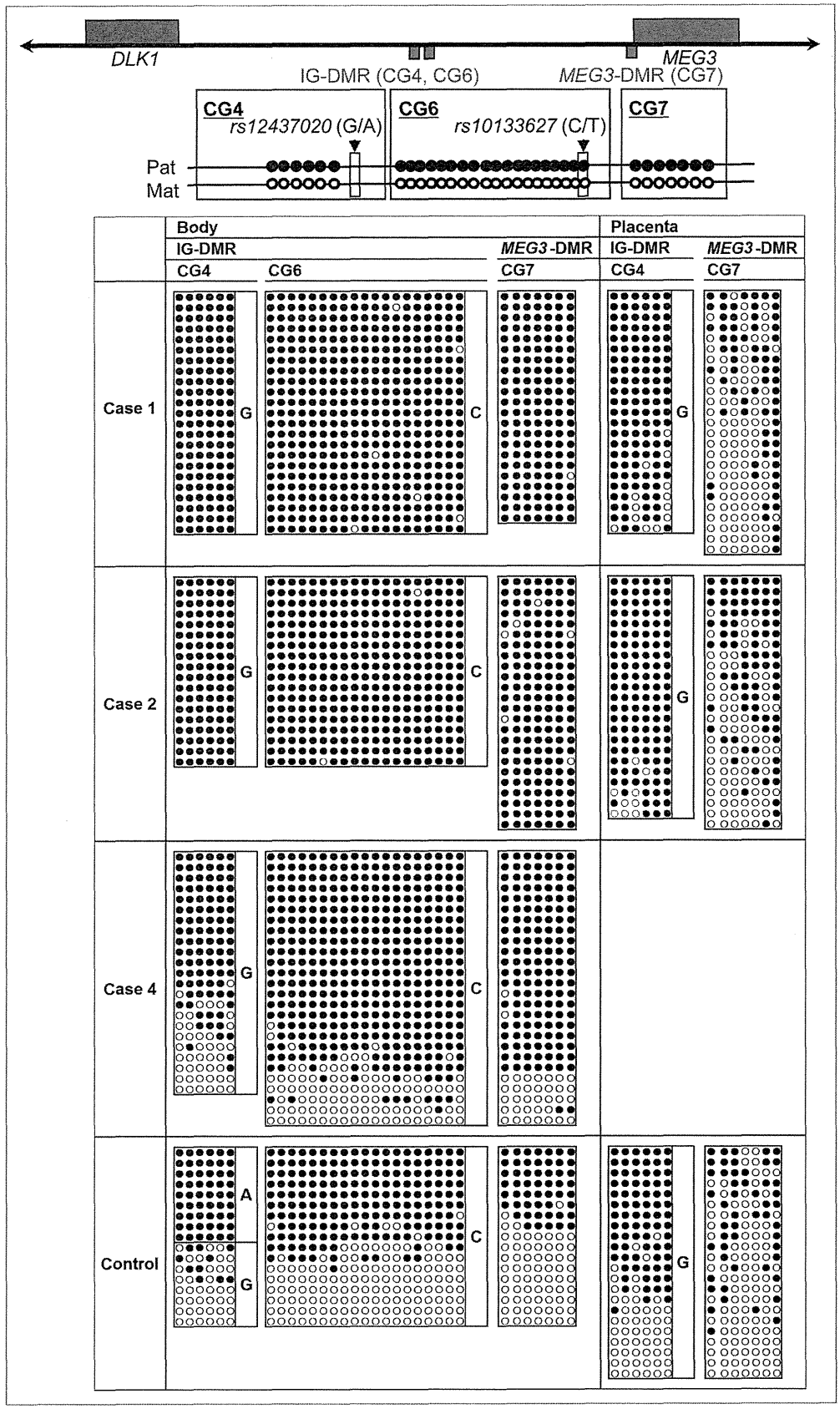

Figure 2. For figure legend, see page 1144.

origin of the der(17) chromosome harboring the chromosome14q32.2 imprinted region. Consistent with this, bisulfite sequencing showed moderate hypermethylation of the IG-DMR and the *MEG3*-DMR (Fig. 2).

Placental histopathological studies. We performed LM and EM studies, and IHC examinations (Fig. 5). LM examinations showed proliferated chorionic villi in cases 1–3. Capillary lumens were irregularly dilated with thickened endothelium in the stem to intermediate villi, but not in the terminal villi. Immature villi were present in case 3, probably because of 30 weeks of gestational age. Chorangioma was also identified in case 3. There was no villous chorangiosis, edematous change of villous stroma, or mesenchymal dysplasia characterized by grapelike vesicles in cases 1–3. Although the terminal villi exhibited no definitive abnormalities in the LM studies, EM examinations revealed swelling of vascular endothelial cells and hypertrophic change of pericytes in the terminal villi, together with narrowed capillary lumens, in cases 1 and 2.

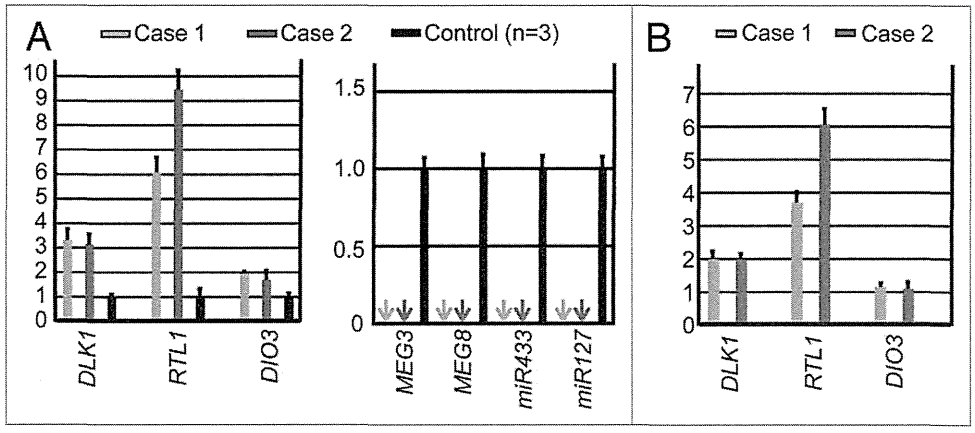

Figure 3. Quantitative real-time PCR analysis using placental samples. For a control, a pooled RNA sample consisting of an equal amount of total RNA extracted from three fresh control placentas was utilized. (**A**) Relative mRNA expression levels for *DLK1*, *RTL1*, and *DIO3* against *GAPDH* (mean ± SE) and lack of *MEGs* expression (indicated by arrows) (*miR433* and *miR127* are encoded by *RTL1as*) in the placental samples of cases 1 and 2. (**B**) Relative mRNA expression levels for *DLK1*, *RTL1*, and *DIO3* against *GAPDH* (mean ± SE), in the equal amount of expression positive placental cells (vascular endothelial cells and pericytes) of cases 1 and 2 (corrected for the difference in the relative proportion of expression positive cells between the placental samples of cases 1 and 2 and the control placental samples, on the assumption that the *DLK1* expression level is "simply doubled" in the expression positive placental cells of case 1 and 2).

IHC examinations identified RTL1, DLK1 and DIO3 protein expressions in the vascular endothelial cells and pericytes of chorionic villi, but not in the cytotrophoblasts, syncytiotrophoblasts, and stromal cells, in the placentas of cases 1–3 and in the control placenta. The PEGs protein expression level was variable in the control placenta, with moderate DLK1 expression, high RTL1 expression, and low DIO3 expression. Furthermore, DLK1 protein expression was apparently stronger in the placentas of cases 1 and 2 than in the placenta of case 3 and the control placenta, RTL1 protein expression was obviously stronger in the placentas of cases 1–3 than in the control placenta, and DIO3 protein expression was apparently similar between the placentas of cases 1–3 and the control placenta.

Discussion

We studied placental samples obtained from cases 1–3 with typical body and placental upd(14)pat phenotype. In this regard, the microsatellite data suggest that upd(14)pat with heterodisomic and isodisomic loci in case 1 was caused by trisomy rescue or gamete complementation, and that upd(14)pat with isodisomic loci alone in case 2 resulted from monosomy rescue or postzygotic mitotic error, although it is possible that heterodisomic locus/loci remained undetected in case 2.[15] Notably, there was no trace of a maternally inherited locus indicative of the presence of trisomic cells or normal cells with biparentally inherited chromosome 14 homologs in the placentas as well as in the leukocytes of cases 1 and 2. In addition, the microdeletion of case 3 has been shown to be inherited from the mother with the same microdeletion.[2] These findings imply that the placental tissues as well as the leukocytes of cases 1–3 almost exclusively, if not totally, consisted of cells with upd(14)pat or those with the microdeletion.

The q-PCR analysis was performed for the fresh placental samples of cases 1 and 2. In this context, two matters should be pointed out. First, the proportion of vascular endothelial cells and pericytes expressing *DLK1*, *RTL1*, and *DIO3* would be somewhat variable among samples, because only a small portion of the placenta was analyzed. This would be relevant to the some degree of difference in the expression levels between the placental samples of cases 1 and 2. Second, the relative proportion of vascular endothelial cells and pericytes expressing *DLK1*, *RTL1*, and *DIO3* would be higher in the placental samples of cases 1 and 2 than in the control placental samples, because the placentas of cases 1 and 2 were accompanied by proliferation of the chorionic villi with such expression positive cells. Thus, it would be inappropriate to perform a simple comparison of relative expression levels against *GAPDH* between the placental samples of cases 1 and 2 and the control placental samples. Indeed, although a complex regulatory mechanism(s), as implicated for the *RTL1* expression,[1,2] is unlikely to be operating for the *DLK1* expression, the relative *DLK1* expression level was 3.3 times and 3.1 times, not 2 times, higher in the placental samples of cases 1 and 2 than in the control placental samples, respectively (Fig. 3A). Assuming that *DLK1* expression level is simply doubled in expression positive cells of cases 1 and 2, it is predicted that the relative proportion of such expression positive cells is 1.65 times (3.3 ÷ 2.0) and 1.55 times (3.1 ÷ 2.0) larger in the placental samples of cases 1 and 2 than in the control placental samples, respectively. Thus, the expression level against *GAPDH*

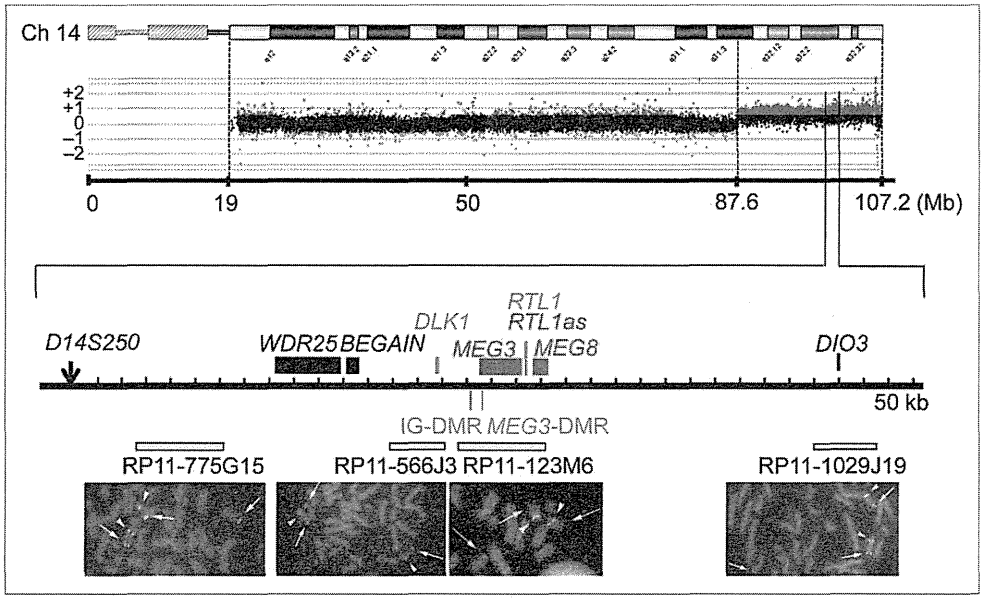

Figure 4. Array CGH and FISH analysis for the distal chromosome 14 region in case 4. In CGH analysis, the black, the red, and the green dots denote signals indicative of the normal, the increased (> +0.5), and the decreased (< −1.0) copy numbers, respectively. In FISH analysis, red signals (arrows) are derived from the probes detecting the various parts of the 14q32.2 imprinted region (the physical positions are indicated with yellow bars), and the green signals (arrowheads) are derived from an RP11–566I2 probe for 14q11.2 used as an internal control.

in the equal amount of expression positive cells is estimated as 3.69 times (6.1 ÷ 1.65) increased for *RTL1* and 1.15 times (1.9 ÷ 1.65) increased for *DIO3* in case 1, and as 6.06 times (9.4 ÷ 1.55) increased for *RTL1* and 1.09 times (1.7 ÷ 1.55) increased for *DIO3* in case 2 (**Fig. 3B**).

Thus, the expression data are summarized as follows (**Fig. 6**). First, it is inferred that the relative *RTL1* expression level is markedly (~5 times) increased in the expression positive cells of the placentas with upd(14)pat, as compared with the control placentas. This degree of elevation is grossly similar to that identified in the body of mice with the targeted deletion of the maternally derived IG-DMR (~4.5 times).[5] Such a markedly increased *RTL1* expression would be explained by assuming that *RTL1as*-encoded microRNAs (e.g., *miR433* and *miR127*) function as a repressor for *RTL1* expression through the RNAi mechanism, as has been indicated for the mouse *Rtl1-Rtl1as* interaction.[16,17] Second, it is unlikely that *DIO3* is solely expressed from the paternally inherited allele, although it remains to be determined whether *DIO3* undergoes partial imprinting like mouse *Dio3*[12] or completely escapes imprinting. In either case, the results would explain why patients with upd(14)pat and upd(14)mat lack clinically recognizable thyroid disorders,[2] although *DIO3* plays a critical role in the inactivation of thyroid hormones.[18]

This study provides further support for a critical role of excessive *RTL1* expression in the development of upd(14)pat phenotype (**Fig. 6**). Indeed, markedly (~5 times) increased *RTL1* expression is shared in common by cases 1–3 with typical upd(14)pat body and placental phenotype. In this context, it is notable that case 4 had no clinically recognizable upd(14)pat body and placental phenotype, except for omphalocele. This would imply that a single copy of *RTL1as* can almost reduce the *RTL1* expression dosage below the threshold level for the development of upd(14)pat phenotype by exerting a trans-acting repressor effect on the two functional copies of *RTL1*. By contrast, the relevance of *DLK1* to upd(14)pat phenotype is unlikely, because case 3 exhibited typical upd(14)pat phenotype in the presence of a single functional copy of *DLK1*, and case 4 showed no upd(14)pat phenotype except for omphalocele in the presence of two functional copies of *DLK1*. Similarly, if *DIO3* were more or less preferentially expressed from paternally inherited allele, the relevance of *DIO3* to upd(14)pat phenotype would also remain minor, if any. Case 4 had no upd(14)pat phenotype except for omphalocele in the presence of with two copies of *DIO3* of paternal origin. It should be pointed out, however, that the absence of *MEGs* expression may have a certain effect on the development of upd(14)pat phenotype.

The placental histological examinations revealed several informative findings. First, DLK1, RTL1, and DIO3 proteins were specifically identified in vascular endothelial cells and pericytes of chorionic villi in the control placenta, with RTL1 protein being most strongly expressed. These results, together with abnormal LM and EM findings of such cells in cases 1–3, suggest that these proteins, especially RTL1 protein, plays a pivotal role in the development of endothelial cells and pericytes. In this regard, it may be possible that the endothelial thickening and resultant narrowing the capillary lumens in the terminal villi have resulted in the dilatation of the stem to intermediate portions of the chorionic villi.

Second, the degree of protein staining was well correlated with the expression dosage of corresponding genes. In this regard, since characteristic macroscopic and microscopic placental features were identified in cases 1–3 who shared markedly elevated RTL1 protein expression, this is consistent with the notion that upd(14)pat phenotype is primarily caused by the markedly

elevated *RTL1* expression.[2] Indeed, DLK1 protein expression was not exaggerated in case 3 with typical upd(14)pat phenotype, and DIO3 protein expression was not enhanced in cases 1–3. It may be possible, however, that the abnormality of placental structures may have resulted in a difference in immunostaining without an actual change in gene expression. This point awaits further investigations.

Third, villous chorangiosis, stromal expansion, and mesenchymal dysplasia were not identified in the placental samples of cases 1–3, although such a lesion(s) may have existed in non-examined portions. Notably, such lesions are frequently observed in placentas of patients with BWS.[19-21] Thus, while both upd(14)pat and BWS are associated with placentomegaly and polyhydroamnios, characteristic histological findings appear to be different between upd(14)pat and BWS.

This study would also provide useful information on the methylation patterns of the *MEG3*-DMR in the placenta. Our previous studies using formalin-fixed and paraffin-embedded placental samples revealed that roughly two-thirds of clones were hypermethylated and the remaining roughly one-third of clones were hypomethylated in case 3 as well as in the previously reported patients with upd(14)pat (not cases 1 and 2) and epimutation (hypermethylation of the IG-DMR and the *MEG3*-DMR of maternal origin), and that roughly one-third of clones were hypermethylated and the remaining roughly two-thirds of clones were hypomethylated in control placental samples (see Fig. S2C in ref. 2). However, this study showed that the *MEG3*-DMR was grossly hypomethylated in the fresh placental samples of cases 1 and 2, with an extent similar to that identified in the fresh control placental samples. In this regard, it is notable that PCR products could be obtained only after 35 cycles for the formalin-fixed and paraffin-embedded placental samples and were sufficiently obtained after 30 cycles for the fresh placental samples. Thus, several specific clones may have been selectively amplified in the previous study. Furthermore, it may be possible that efficacy of bisulfite treatment (conversion of unmethylated cytosine into uracils and subsequently thymines) may be insufficient for the formalin-fixed and paraffin-embedded placental samples. Thus, it appears that the present data denote precise methylation patterns of the *MEG3*-DMR in the placenta.

In summary, the present study provides useful clues for the clarification of regulatory mechanism for the *RTL1* expression, imprinting status of *DIO3* and characteristic placental histological findings in patients with upd(14)pat and related conditions. Further studies will help improve our knowledge about upd(14)pat and related conditions.

Methods

Ethical approval. This study was approved by the Institutional Review Board Committees of each investigator, and performed after obtaining written informed consent.

Primers. Primers utilized in this study are summarized in Table S3.

Sample preparation for molecular studies. Genomic DNA samples were obtained from leukocytes using FlexiGene DNA Kit (Qiagen) and from placental samples using ISOGEN (Nippon Gene). Transcripts of *DLK1, MEG3, RTL1, MEG8* and *DIO3* were isolated with ISOGEN (Nippon Gene), and *microRNAs* were extracted with mirVana™ miRNA Isolation Kit (Ambion). After DNase treatment, cDNA samples for *DLK1, MEG3, MEG8* and *DIO3* were prepared with oligo(dT) primers from 1 μg of RNA using Superscript III Reverse Transcriptase (Invitrogen), and those of *microRNAs* were synthesized from 300 ng of RNA using TaqMan MicroRNA Reverse Transcription Kit (Applied Biosystems). For *RTL1*, 3'-RACE was utilized to prevent amplification of *RTL1as*; cDNA was synthesized from 1 μg of RNA using Superscript III Reverse Transcriptase with a long primer hybridizing to poly A site and introducing the adaptor sequence. Lymphocyte metaphase spreads for FISH analysis were prepared from leukocytes using colcemide (Invitrogen).

Molecular studies. Microsatellite analysis for 19 loci on chromosome 14, methylation analysis for the IG-DMR and

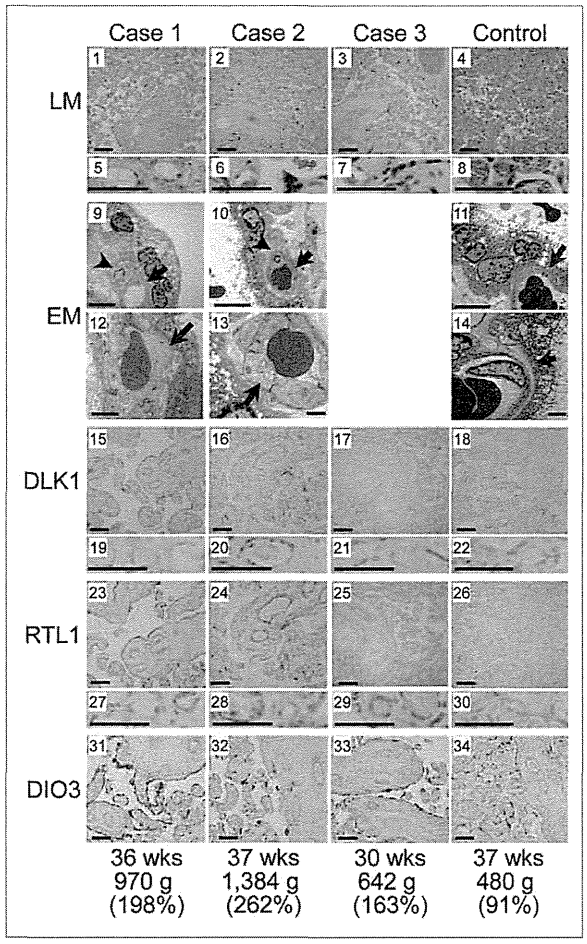

Figure 5. Histological examinations. LM, light microscopic examinations; EM, electron microscopic examinations; DLK1, RTL1 and DIO3, immunohistochemical examinations for the corresponding proteins. The arrows and arrowheads in the EM findings indicate endothelial cells and pericytes, respectively. Scale bars represent 100 μm for 1–4, 15–18, 23–26 and 31–34, 50 μm for 5–8, 19–22 and 27–30, 5 μm for 9–11 and 2 μm for 12–14. Gestational age, placental weight, and % placental weight assessed by the gestational age-matched Japanese references for placental weight[4,22] are described.